AN ABSTRACT OF THE THESIS OF

Christopher Jackson Herring for the degree of Doctor of Philosophy in Chemistry presented on September 30, 1996.
Title: A New Glow Discharge Detector for Carbohydrates in Aqueous Chromatography.

Abstract approved: Redacted for Privacy

Edward H. Piepmeier

An atmospheric pressure argon glow discharge is shown to detect trace levels of carbohydrates in aqueous flowing systems, using either of two glow discharge solution interface configurations. The first configuration consists of an oscillating glow discharge sustained between a flowing aqueous cathode and platinum anode. Picomole and micromolar mass and concentration detection limits, respectively, are obtained for sucrose in an aqueous flow injection system when monitoring discharge oscillation frequency or discharge current. The second configuration consists of a non-oscillating glow discharge sustained between metallic electrodes near the flowing output of a high performance liquid chromatography system. A conductivity detector detects the acidic product formed when each carbohydrate elutes and is exposed to the glow discharge. This detector yields femtomole and nanomolar mass and concentration

detection limits, respectively, for a variety of carbohydrates and competes with the best of the commercially available liquid chromatography carbohydrate detectors. An increase in the discharge electrode spacing or reduction in the liquid flow rate increases detector sensitivity, since the discharge area and solution exposure time are increased, respectively. The aqueous carbohydrate products formed from exposure to the glow discharge are similar to those formed from exposure to high energy radiation. Acid, hydrogen peroxide, and an absorbing species all form in amounts proportional to carbohydrate concentration and glow discharge exposure time, with yields approximating those encountered when using high energy radiation.

A New Glow Discharge Detector for Carbohydrates in Aqueous Chromatography

by

Christopher Jackson Herring

A THESIS

submitted to

Oregon State University

in partial fulfillment of
the requirements for the
degree of

Doctor of Philosophy

Presented September 30, 1996
Commencement June, 1997

Doctor of Philosophy thesis of Christopher Jackson Herring presented on September 30, 1996

APPROVED:

Redacted for Privacy

Major professor, representing Chemistry

Redacted for Privacy

Chair of Department of Chemistry

Redacted for Privacy

Dean of Graduate School

I understand that my thesis will become part of the permanent collection of Oregon State University libraries. My signature below authorizes release of my thesis to any reader upon request.

Redacted for Privacy

Christopher Jackson Herring, Author

ACKNOWLEDGEMENT

I would like to thank Dr. Edward H. Piepmeier for his guidance and support during my time at Oregon State University. I have enjoyed working in his laboratory.

I would also like to thank Dr. Ingle, Dr. Loeser, Dr. Schuyler, and Dr. Zabriskie for serving on my committee.

In addition I would like to thank Kevin Cantrell, Zhubiao Zhu, Diane Smith, Brian Jones, Paul Bacon, and Ying Yang for their friendship.

Most importantly I would like to thank my parents Betty and Jack Herring for their constant support and guidance.

Finally I would like to thank my wife Nazy Khosrovani for her love, support, and patience.

TABLE OF CONTENTS

TABLE OF CONTENTS (Continued)

TABLE OF CONTENTS (Continued)

LIST OF FIGURES

LIST OF FIGURES (Continued)

LIST OF FIGURES (Continued)

Figure **Page**

A NEW GLOW DISCHARGE DETECTOR FOR CARBOHYDRATES IN AQUEOUS CHROMATOGRAPHY

Chapter 1
Introduction

1.1 Plasmas

A plasma is an electrically neutral ionized gas consisting of equivalent numbers of positive ions and electrons. There are many types of plasmas and over 99% of the universe is considered to be in the plasma state.[1] Plasmas are classified by the densities and temperatures at which they exist. For example, solar wind plasmas exist at extremely low temperatures and pressures while nuclear fission plasmas exist at extremely high temperatures and pressures. Other plasmas such as the Aurora Borealis, solar corona, flame, arc, glow discharge, and Townsend discharge exist inbetween these two extremes. Important properties of plasmas include their ability to conduct electricity and interact with external magnetic and electric fields. Also, the highly energetic plasma environment can induce many unique processes such as plasma polymerization, plasma etching, plasma deposition, and various chemical reactions.

1.2 The Glow Discharge

The glow discharge is one of the most widely studied forms of plasma. While the first observations of glow discharge phenomena date back to the early seventeenth century[2] the detailed scientific examinations, which led to significant advancements in physics, began in the nineteenth century.[3-7]

In the laboratory, the glow discharge is initiated by applying high voltage between a metallic cathode and anode. The discharge may operate in any gas but the most commonly used gases are highly purified inert gases such as argon and helium, as well as nitrogen. The discharge operating pressure is typically a few Torr (200 Pa) but under the correct circumstances it can be operated at atmospheric pressure.[8] The strong electric field between the electrodes accelerates electrons and positive ions, initially caused by cosmic ionization[8], towards the anode and cathode, respectively. The electrons eventually reach velocities sufficient to ionize gas atoms, causing an electron avalanche in which one positive ion and electron are formed from every gas atom ionized. This avalanche grows until the discharge current becomes limited by the external current limiting resistor.

Due in part to high electron mobilities a positive space charge develops near the cathode resulting in a large potential drop (100-200 V) just in front of the cathode. This region is called the cathode dark space and is critical

to the maintenance of the glow discharge. In this region positive ions are continuously accelerated to bombard the cathode, liberating electrons. These electrons are accelerated towards the anode causing ionization in the cathode dark space. In general, in order to have a self-sustaining glow discharge the potential of the cathode dark space must be such that each electron leaving the cathode causes enough ionization for its replacement by positive ion bombardment.[9] The cathode dark space is followed by the intensely luminous negative glow region. The bright glow is caused by atomic or molecular excitation induced by electron impact. It is a field free region where the numbers of electrons and ions are approximately equal. In this region the electrons lose their energy through ionization and excitation but there is no field to reaccelerate them. Thus the luminosity of this region gradually fades away towards the anode forming the Faraday dark space. In this region there is no ionization or excitation but there is a slight electric field gradient which again accelerates the electrons towards the anode. The positive column starts when the electrons have attained enough energy to excite gas atoms. The positive column is usually the largest part of a glow discharge[10] and behaves most like a plasma, since the densities of positive ions and electrons are equal. The majority of current in the positive column is carried by electrons due to their high velocities and mobilities. Electrons can, however, be lost from the positive column by

diffusion and collisions, thus there exists a slight potential gradient in the positive column to regenerate or reaccelerate these electrons. Towards the end of the positive column the electrons have attained enough energy to mainly ionize. This region of low luminosity is called the anode dark space and typically has a potential drop on the order of the ionization potential of the gas. The electrons in the anode region must liberate enough positive ions (through ionization) to account for the ions flowing out of the cathode end of the positive column. This includes ions lost to diffusion in the positive column. Electrons accelerating through the anode dark space eventually lose energy from collisions, and the resulting slow electrons then cause excitation forming the anode glow, very near to the anode surface.

The formation of the above regions is virtually instantaneous and an overall equilibrium is reached when the rate of ionization in the discharge is equal to the rate of recombination. The discharge is very stable and consumes very little power with currents typically in the milliamp region.[8,10,11] The glow discharge may be operated with the cathode completely covered by the discharge (abnormal mode) or incompletely covered (normal mode). Most glow discharges operate in the abnormal mode and an increase in current results in an increase in current density rather than an increase in cathode surface coverage.

Under certain operating conditions the current in a glow discharge may oscillate. Such oscillations have been known for some time[11-15] but the exact mechanism of formation is not completely understood. Oscillations can occur in the cathode dark space, positive column, and anode dark space at frequencies ranging from a few hertz to many megahertz.

1.3 Glow Discharge Applications

The glow discharge is one of the most important forms of plasma in analytical chemistry. A very desirable feature of the glow discharge is that it is able to generate large populations of atoms from a sample in both excited and ionized states. Thus the glow discharge has been used extensively in the direct elemental analysis of solids using atomic absorption[16], emission[17], fluoresence[18,19], and mass spectroscopies.[20-23] A glow discharge has also been used as an ionization source for liquid chromatography mass spectrometry.[24-27]

In the 1950's the first low pressure glow discharge detector for gas chromatography was developed, where glow discharge voltage was monitored as a function of time.[28,29] Recently, a new oscillating glow discharge detector was developed for gas chromatography where oscillation frequency and discharge current were monitored to obtain sensitive determinations, and structurally significant information for a variety of organic compounds.[30-32]

To date, however, there have been no studies focusing on the use of a glow discharge for detection in liquid separation techniques such as liquid chromatography and capillary electrophoresis. There has been, however, some work done on the on-line determination of various metals in aqueous flowing systems by monitoring the emission of a liquid-interfaced atmospheric pressure glow discharge.[33,34]

1.4 Glow Discharge Electrolysis

Numerous authors[35-38] have performed glow discharge electrolysis experiments where the discharge is formed by raising a metallic anode above a conducting liquid cathode. In such experiments solution species are typically oxidized in excess of that predicted by Faraday's law. Such oxidation has been explained by the discharge induced creation of highly oxidizing OH radicals formed in solution due to water dissociation from ion impact. The excess oxidation is balanced by an equivalent amount of hydrogen gas production (reduction), and hydrogen peroxide is also formed. Most studies have focused on aqueous solutions containing various metal ions and no work has investigated the transformations induced in important organic compounds such as carbohydrates and proteins.

It has been determined that glow discharge electrolysis induces solution reactions which are similar to those encountered when the same solutions are exposed to high energy radiation.[35-38] For example, aqueous solutions exposed

to a liquid-interfaced glow discharge or high energy radiation both yield excess substrate oxidation and the generation of hydrogen peroxide and hydrogen gas. Unlike the glow discharge electrolysis studies, there have been numerous studies which have investigated the products formed when aqueous organic compounds are exposed to high energy radiation.[39-45] One of the most widely studied groups of compounds are the carbohydrates. It has been found that exposure of any aqueous carbohydrate to high energy radiation yields a very complicated mixture of oxidation products including acids, deoxy- and deoxyketo-compounds, and various UV absorbing species. It has been confirmed that most of the oxidation is due to the radiation induced formation of aqueous hydroxyl radicals which react rapidly with all carbohydrates.

1.5 Research Goal

The primary goal of this research is to develop a liquid chromatography detector, somehow implementing an atmospheric pressure glow discharge, which detects trace levels of carbohydrates. Ideally the detector should have higher or comparable sensitivity to the commercially available liquid chromatography carbohydrate detectors, and should also be compatible with common mobile phases used in the analysis of carbohydrates.

Carbohydrates are a very important class of compounds that have numerous biologically significant roles.[46,47] The

recent interest in carbohydrate moieties attached to glycoproteins has increased the need for more sensitive carbohydrate detectors. In fact, it has been found that the detection limit of the analytical method needs to be submicromolar[48] due to low amounts of the initial glycoprotein. This is currently challenging the most sensitive commercially available carbohydrate detector, the pulsed amperometric detector, which has detection limits in the nanomolar range.

The first part of this thesis describes the development of a liquid-interfaced oscillating glow discharge detector for sucrose in an aqueous flow injection type system. A description of the visual appearance of the glow discharge floating on the flowing eluent is given along with various parameters which affect oscillation and current stability. The sensitivity and linearity of this detector is also discussed.

In the second part of the thesis a new glow discharge-conductivity detector for carbohydrates is described in detail. The linear range, sensitivity, and sensitivity controlling parameters such as liquid flow rate, electrode spacing, discharge current, and discharge area are described. It is shown that the detector exhibits the sensitivity and other characteristics necessary to compete with the pulsed amperometric detector. In addition it is explained how the sensitivity and linear range may be further improved by using large area glow discharges or

multiple parallel glow discharges. Finally, it is shown that the detector is compatible with aqueous ligand exchange chromatography, which is a relatively new and desirable means of separating carbohydrates.

1.6 References

[1] Eliezer, Yaffa; Eliezer, S. *The Fourth State of Matter: An Introduction to the Physics of Plasma*, Adam Hilger: Philadelphia, 1989.

[2] Gilbert, W., De Magnete, *Magneticisque Corporibus*, Petrus Short, London, 1600.

[3] Faraday, M., *Res. Elec.*, 1839, 663.

[4] Crookes, W., *Phil. Trans.*, Pt. I, 1879b, p. 152.

[5] Hittorf, J.W., *Pogg. Ann.*, 1869, 136, 8.

[6] Davy H. *Phil. Trans.*, 1821, 111, 427.

[7] Goldstein, E., *Berl. Monat.*, 1876, 283.

[8] Nasser, Essam, *Fundamentals of Gaseous Ionization and Plasma Electronics*, Wiley-Interscience: New York, 1971.

[9] Penning, F.M., *Electrical Discharges in Gases*, The Macmillan Company: New York, 1957.

[10] Marcus, R.K., *Glow Discharge Spectroscopies*, Plenum Press: New York, 1993.

[11] Petrovic Z.L.; Phelps, A.V., *Phys. Rev.*, 1993, 47, 2806.

[12] Jelenkovic, B.M.; Rozsa, K.; Phelps, A.V., *Phys. Rev.*, 1993, 47, 2816.

[13] Phelps, A.V.; Petrovic. Z.L.; Jelenkovic. B.M., *Phys. Rev.*, 1993, 47, 2825.

[14] Donahue, T.; Dieke, G.H., *Phys. Rev.*, 1951, 81, 248.

[15] Zhubiao, Z: Piepmeier, E.H., *Spectrochim. Acta*, 1994, 49B, 1787.

[16] Ohls, K.; Flock, J.; Loepp, H. *Fresenius Z. Anal. Chem.*, 1988, 332, 456.

[17] Broekaert, J.A.C., *J. Anal. At. Spectrom.* 1987, 2, 537.

[18] Smith, B.W.; Womack, J.B.; Omenetto, N.; Winefordner, J.D. *Appl. Spectrosc.*, 1989, 43, 873.

[19] Smith, B.W.; Omenetto, N.; Winefordner, J.D., *Spectrochim. Acta*, 1984, 39B, 1389.

[20] Stuewer, D. *Fres. J. Anal. Chem.*, 1990, 337, 737.

[21] Carazzato D.; Bertrand, M.J. *J. Am. Soc. Mass Spect.*, 1994, 5, 299.

[22] McLuckey, S.A.; Glish, G.L.; Asano, K.G.; Grant, B.C. *Anal. Chem.*, 1988, 60, 2220.

[23] Harrison, W.W.; Hess, K.R.; Marcus, R.K. *Anal. Chem.*, 1986, 58, 341A.

[24] Bellar, T.A.; Budde, W.L.; Kryak, D.D. *J. Am. Soc. Mass Spect.* 1994, 5, 908.

[25] Ratliff, P.H.; Harrison, W.W. *Spectrochim. Acta* 1994, 49B, 1747.

[26] Barshick, C.M.; Duckworth, D.C.; Smith, D.H. *J. Am. Soc. Mass Spect.* 1993, 4, 38.

[27] Zhao, J.; Zhu, J.; Lubman, D.M. *Anal. Chem.*, 1992, 64, 1426.

[28] Harley, J.; Pretorius, V. *Nature*, 1956, 178, 1244.

[29] Pitkethly, R.C. *Anal. Chem.*, 1958, 30, 1309.

[30] Kuzuya, M.; Piepmeier, E.H. *Anal. Chem.*, 1991, 63, 1763.

[31] Smith, D.L.; Piepmeier, E.H. *Anal. Chem.*, 1994, 66, 1323.

[32] Smith, D.L.; Piepmeier, E.H. *Anal. Chem.*, 1995, 67, 1084.

[33] Cserfalvi, T.; Mezei, P. J. *Anal. Atomic Spect.*, 1994, 9, 345.

[34] Cserfalvi, T.; Mezei, P.; Apai, P. J. *Appl. Phys. D.*, 1993, 26, 2184.

[35] Denaro, A.R.; Hickling, A., *J. Electrochem. Soc.*, 1958, May, 265.

[36] Hickling, A.; Ingram, M.D., *J. Electroanal. Chem.*, 1964, 8, 65.

[37] Denaro, A.R.; Owens, P.A., *Electrochim. Acta*, 1968, 13, 157.

[38] Dewhurst, H.A.; Flagg, J.F.; Watson, P.K., *J. Electrochem. Soc.*, 1959, April, 366.

[39] Bothner-By, C.T.; Balazs, E.A., *Rad. Res.*, 1957, 6, 302.

[40] Phillips, G.O., *Rad. Res.*, 1963, 18, 446.

[41] Wolfrom, W.L.; Binkley, W.W.; McCabe, L.J.; Han, T.M.; Michelakis, A.M., *Rad. Res.*, 1959, 10, 39.

[42] Phillips, G.O.; Griffiths, W.; Davies, J.V., *J. Chem. Soc.*, 1966, 194.

[43] Allen, A.O., *The Radiation Chemistry of Water and Aqueous Solutions*, D. Van Nostrand Company, Inc.: New York, 1961.

[44] Kochetkov, N.K.; Kudrjashov, L.I.; Chlenov, M.A., *Radiation Chemistry of Carbohydrates*, Pergamon Press: New York, 1979.

[45] Spinks, J.W.T.; Woods, R.J., *An Introduction to Radiation Chemistry*, Third Edition, John Wiley & Sons, Inc.; New York, 1990.

[46] Sharon, N.; Lis, H., *Sci. Amer.*, 1993, Jan., 82.

[47] Paulson, J.C., *TIBS 14*, 1989, July, 272.

[48] Paulus, A.; Klockow, A., *J. Chromatogr. A.*, 1996, 720, 353.

Chapter 2

A Liquid Interfaced Oscillating Glow Discharge Detector For a Flowing Liquid System

Christopher J. Herring and Edward H. Piepmeier

Published in *Analytical Chemistry*
(Vol. 67, No. 5, p. 878-884, 1995)

2.1 Abstract

A new liquid-interfaced oscillating glow discharge detector having a frequency and current response to femtomole and picomole quantities, respectively, of potassium nitrate and sucrose injected into an aqueous flowing eluent is presented. The glow discharge is formed in an argon atmosphere at ambient pressure between a platinum anode and a cathode consisting of an aqueous conducting solution. A detailed description of the appearance of the liquid-interfaced glow discharge at various electrode distances and the occurrence of high frequency oscillations is given.

2.2 Introduction

It has been known for over a century that conduction between a metallic electrode and liquid surface can be accomplished using an electrical gas discharge where one electrode is raised above a conducting solution containing the other electrode[1]. Hickling and other authors have carried out extensive studies of what they have termed "glow discharge electrolysis" and have established its similarities to radiation chemistry where highly reactive species are produced in the liquid phase.[1-3] The[2,3] same authors have shown that the reactive species generated cause substrate oxidation in excess of that predicted from Faraday's laws and have proposed extensive reaction mechanisms to explain the excess oxidation.[1-5]

The majority of glow discharge electrolysis studies have been carried out under reduced pressures and use a nonreplenishing catholyte volume where no new electrolyte solution is introduced. Recently, however, it was shown that an atmospheric pressure glow discharge can be used as an emission source for the direct determination of metals in aqueous solution.[6]

The purpose of this paper is to demonstrate that oscillation frequency and current signals in an atmospheric pressure glow discharge, occurring between a platinum anode and aqueous cathode, can be used as a means of detecting both ionic and nonionic species in a flowing liquid system.

Studies of oscillations occurring in reduced pressure glow discharges using metallic electrodes have been recorded extensively in the literature,[7,8] but to date no study has reported the presence of high frequency oscillations in an atmospheric pressure glow discharge between a metallic and liquid electrode.

Recent work with an oscillating glow discharge detector for gas chromatography shows universal response and low detection limits for a variety of compounds.[9] It is hoped that the liquid- interfaced oscillating glow discharge detector presented in this paper will eventually become a sensitive universal detector for flowing liquid systems.

2.3 Experimental

2.3.1 Detector Cell

The glow discharge detector cell is shown in Figure 2.1. The cell body consists of a 3/8-in. brass Ultra-Torr union tee with a fourth port consisting of a 3/8-in. Ultra-Torr adapter brazed to a 1/4-in. hole drilled in the bottom center of the tee. Three micrometer stages are used for X, Y, and Z electrode alignment. The above configuration rests on a steel baseplate supported by an intertube which reduces mechanical vibrations from the laboratory.

2.3.2 Liquid Reservoir Setup

Two 1000-mL Pyrex tubulation type Erlenmeyer flask reservoirs with magnetic stirring bars are located 30 cm above the top of the cell. Each flask is fitted with a rubber stopper with a total of 80 cm of 1/16-in.-o.d. x 0.020-in.-i.d. PEEK (poly(ether ether ketone)) tubing is inserted through the stopper so that 10 cm of tubing is submerged beneath the liquid surface. A helium sparging tube is also fitted through each stopper. Sparging helium (99.99 %) is supplied through an in-line oxygen trap (Alltech, Oxy-purge) and a 1/4-in. 0.5-μm Nupro Series F in-line gas filter from a tank equipped with a two stage regulator. Both flasks rest on a steel plate supported by an intertube to reduce vibrations. Liquid levels of the

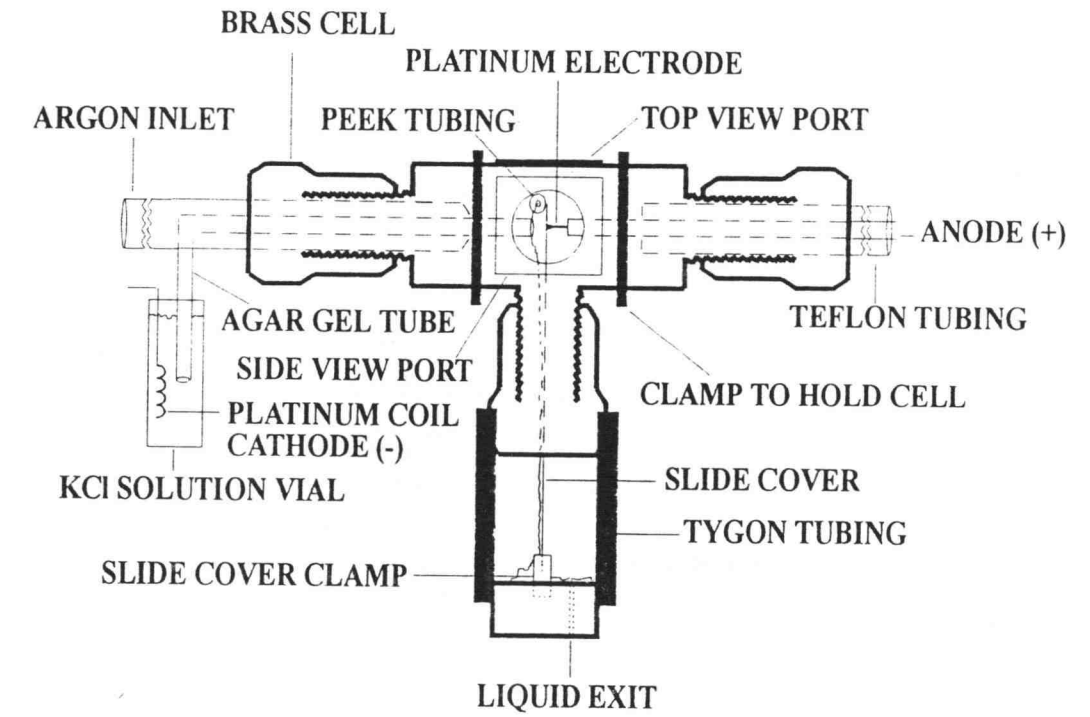

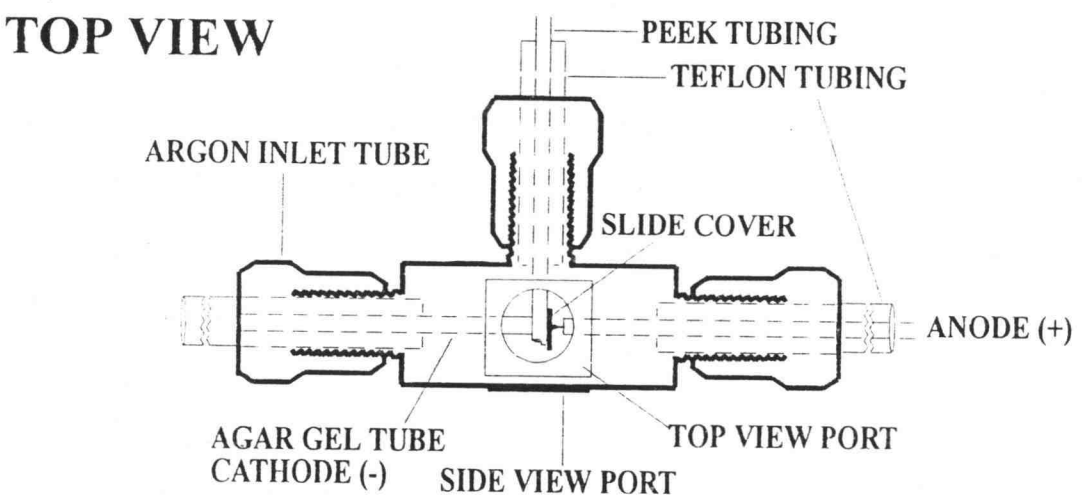

Figure 2.1. Schematic diagram of the glow discharge cell.

eluent and sample flasks are equal, resulting in equal liquid flow rates.

Both lengths of PEEK tubing are connected to a three way slider valve (Rheodyne, 0.8 mm bore, Model 0804A) for sample injection (Figure 2.2). PEEK tubing connects the valve to the detector cell via an Ultra-Torr adapter. With the given configuration a flow rate of approximately 0.42 mL/min is produced.

2.3.3 Liquid Interface

In approximately the center of the cell, the PEEK tubing from the slider valve touches one side of a rectangular 3- x 60- x 0.5-mm glass piece cut from a Corning microscope slide cover held in place by a miniature clamp (Figure 2.3). The rectangular slide cover has a 1/32-in.-diameter hole approximately 0.2 cm from its top and 0.15 cm from either side, enabling the formation of a stable film of eluent across the hole on the side opposite the anode. The liquid film has the same geometry as that of the hole with a slight bulge outwards and provides a very stable sampling region with minimal flow instabilities.

2.3.4 Electrode Configuration

The negative terminal of the high-voltage power supply is connected to a cathode immersed in a solution of saturated KCl. The cathode consists of a coiled 0.02-in.-diameter platinum wire soldered to a 1/16-in.- i.d. x 1/8-

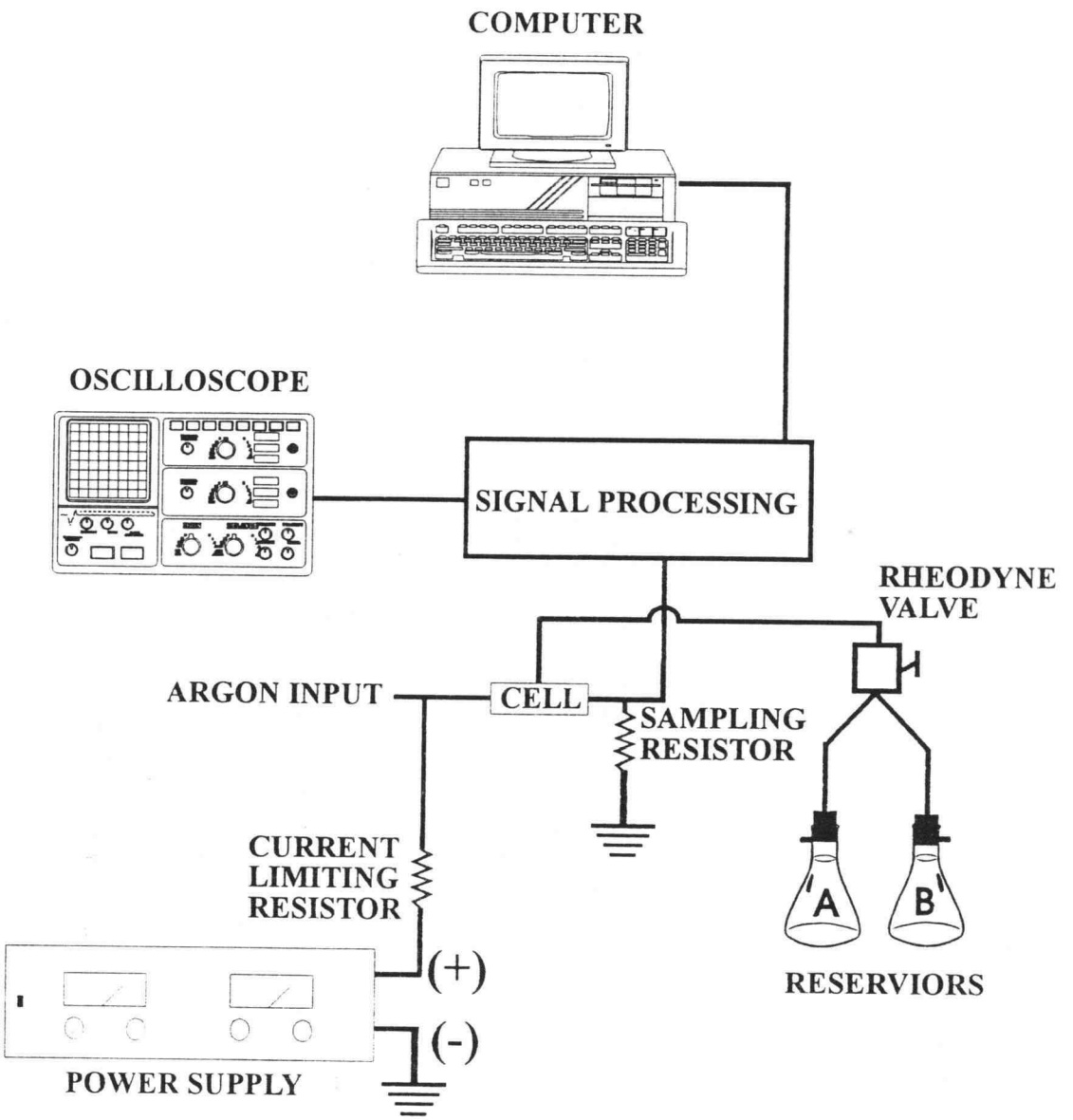

Figure 2.2. Schematic diagram of experimental setup.

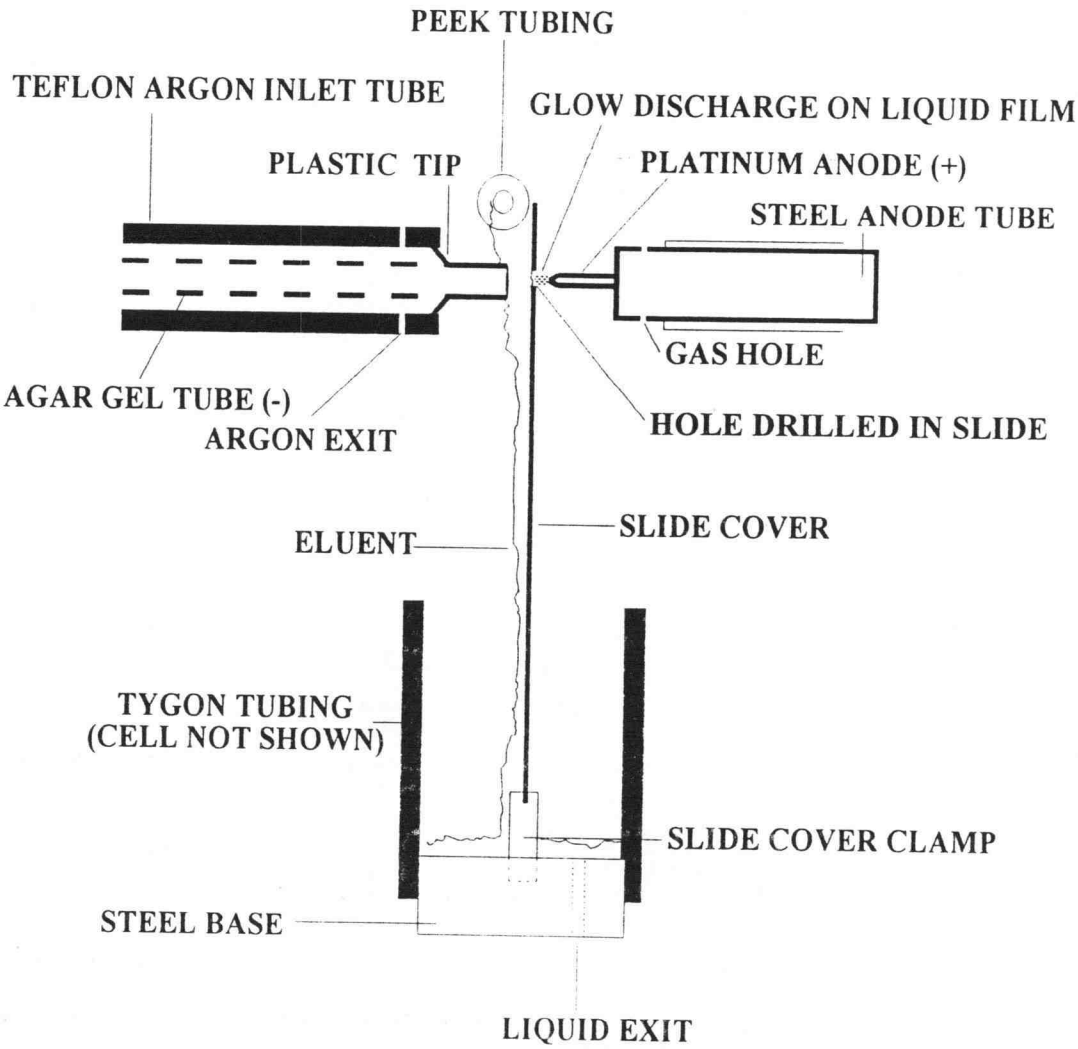

Figure 2.3. Electrode arrangement interfaced to flowing eluent.

in.-o.d. x 2-in.-length stainless steel tube press fit onto the cathode. A Teflon tube filled with a conducting agar gel is used to connect the potassium chloride solution to the flowing stream of eluent in the detector cell. This prevents the formation of hydrogen bubbles in the eluent. Approximately 2 mm from the end of the argon inlet tube, four 1/32-in.-diameter holes are drilled at 90° angles to one another allowing argon to flow into the cell.

The anode in the plasma gas consists of a 0.02-in.-diameter x 0.2-in.-length platinum wire soldered on one end to a sealed 1/8-in.-o.d. x 1/16-in.-i.d. x 6-in.-length stainless steel tube. Approximately 0.25 cm from the sealed end are four 1/32-in. holes drilled in the tube side for argon exit. The platinum wire tip has a cone shape with an approximate angle of inclination of 15°. This angle provides the greatest discharge stability.

The platinum anode is positioned on the side opposite the eluent flow and directly centered on the hole in the cover slide, as shown in Figure 2.3. The agar gel tube is submersed in the liquid flow on the side opposite the anode and centered on the hole in the cover slide. In this way, the flowing liquid becomes the cathode for the oscillating plasma. A magnification factor of 100x is provided by a microscope equipped with a calibrated microruler with a resolution of 0.004 mm / division.

2.3.5 Solution Preparation

Reservoir solutions were prepared in doubly deionized water, and all chemicals used were of analytical reagent grade. Solutions were filtered through 0.2-μm filter paper (Rainin, Nylon-66) and then sparged with helium for approximately 10 min. Sodium chloride was chosen as the electrolyte because it is a strong electrolyte, is readily available, and is nontoxic.

2.3.6 Sample Injection Technique

The Rheodyne valve (Figure 2.2) is used manually to introduce a small plug of analyte into the eluent by switching between reservoirs A and B for a selected period of time. Switching between reservoirs creates a temporary change in the liquid flow, producing spikes in the current and frequency signals. The exact time period is obtained by measuring the time between the two switching spikes produced in the frequency or current. From this time and the flow rate, the mass of analyte entering the cell is calculated. For all injections, a blank run was run, and no change in the frequency or current baseline was noted. The liquid flow rate was 0.42 ml/min.

2.3.7 Argon Delivery

The Argon gas (99.99 %) is supplied from a tank with a two-stage regulator to a calibrated Matheson 602 flow meter. The flowmeter connects to a 1/4-in., 0.5-μm Series F Nupro

in-line gas filter. The argon stream interfaces to the Teflon tubing, part of which encloses the agar gel tube and extends into the cell through an Ultra-Torr adapter as shown in Figure 2.1. Typical argon flow rates through the cell are 200-500 mL/min.

2.3.8 Electronics

The glow discharge is powered by a regulated, adjustable 2000-V dc (Model 204, Pacific Precision Instruments) high voltage negative power supply. A 655.7-kΩ resistor connected in series between the negative terminal of the power supply and cathode limits the current. A 1-kΩ sampling resistor placed between power supply ground and the anode is used to monitor oscillation and current signals. A digital mulitmeter is placed in series with the circuit to monitor the average current.

Glow discharge oscillations are observed with a digital storage oscilloscope connected to the anode side of the sampling resistor. The anode signal enters a follower-with-gain-of-two, high-speed, low-noise operational amplifier circuit (844AN), followed by a high pass filter with a cutoff frequency of 5 MHz. The signal enters another follower-with-gain-of-two operational amplifier circuit (844AN). The output of this circuit is connected via a 100-Ω resistor to a series of two JK flip flops (DM7473N), which divide the frequency by 4. This output is connected to a Schmitt trigger (74S132N). The TTL signal is sent to the

counting input of counter 0 (8254, 16 bit counter) on a DASH-8 computer interface board. Counter 2 of the DASH-8 is set to have a 100-Hz output, which is divided down using an external divide by 10 counter (SN74161N). This signal is connected to a SN7406N inverter whose output impedance matches the cable impedance. The 10-Hz signal is sent to the gating input of counter 0, which is configured so that it counts during a 90-ms gate time followed by a 10-ms off time every 0.1 s. To allow counts above 65,536 (16 bits, 728177 Hz) the output of counter 0 is fed to the input of counter 1. A Quickbasic computer program monitors counters 0-2 and stores and manipulates the frequency data.

The current is monitored on the anode side of the sampling resistor, to which is connected an inverter with gain-of-two op-amp circuit followed by an RC low-pass filter with a time constant of 0.01 s (one tenth of the 0.1-s sampling time interval). The signal is sent to a gain-of-two operational amplifier circuit whose output is connected to the 12-bit ADC on the DASH-8 board. The current and frequency circuit is surrounded with a Faraday cage to reduce noise.

2.4 Results and Discussion

2.4.1 Liquid Cathode Glow Discharge Ignition

Prior to glow discharge ignition with electrode distances longer than 0.2 cm and an applied voltage of

approximately 1000 V, there appears a very faint whitish glow around the tip of the platinum anode, with no visible glow between the electrodes. Currents in this region are in the microampere range, and the cell voltage is approximately equal to the applied voltage, thus resembling the classical low-current, high-cell voltage Townsend discharge.[10]

The atmospheric pressure glow discharge is initiated by moving the anode towards the liquid cathode surface until visible breakdown occurs. Starting the glow discharge always produces a momentary surge of liquid towards the anode, and occasionally liquid will swell from the film towards the anode and extinguish the discharge. Ignition typically occurs at an electrode spacing of approximately 0.2 cm and an applied voltage of 1000 V, resulting in an electric field strength of 5000 V/cm between the anode and liquid cathode. Discharge currents and cell voltages may range from 0.2 to 1.2 mA and 210 to 420 V, respectively.

2.4.2 Liquid Cathode Glow Discharge Features

To the naked eye, the glow discharge is barely visible, and in general with electrode distances below 0.2 cm, it appears as a bright blue dot on the surface of the liquid. With a magnification factor of approximately 100x, it is evident that the discharge contains many of the standard regions of a classical glow discharge between metallic electrodes under reduced pressure. The Aston dark space, cathode glow, negative glow, Faraday dark space, positive

column, anode dark space, and anode glow have been observed and identified in order of their appearance and color at electrode distances greater than approximately 0.05 cm. The only region not visible is the cathode dark space, but since this is not a completely dark region, it may be obscured by the intense luminosity of the adjacent cathode and negative glows. The color of the cathode glow, negative glow, and positive column (when present) correspond to that expected for the same regions in an argon glow discharge at reduced pressure.[10]

It is possible to sustain the glow discharge over a range of electrode distances and liquid flow rates ranging from 8 μm to 1 cm and 50 μL to 2 ml/min, respectively.

Visual discharge stability decreases with electrode distances greater than approximately 0.5 cm. Visual discharge instabilities appear as rapid fluxuations in the whole discharge or as wandering at either electrode. In some cases, the discharge may branch to many places on the liquid at once. Argon flow rates which result in a visually stable glow discharge vary from 200 to 500 mL/min, with current increasing as flow rate increases.

2.4.3 Behavior at Electrode Distances Above 0.01 cm

Figure 2.4 shows the appearance of the glow discharge with electrode spacings greater than 0.01 cm. In general, when the electrode distance is greater than 0.01 cm, the pinkish cathode glow appears as a luminous disk near the

NONOSCILLATING GLOW DISCHARGE

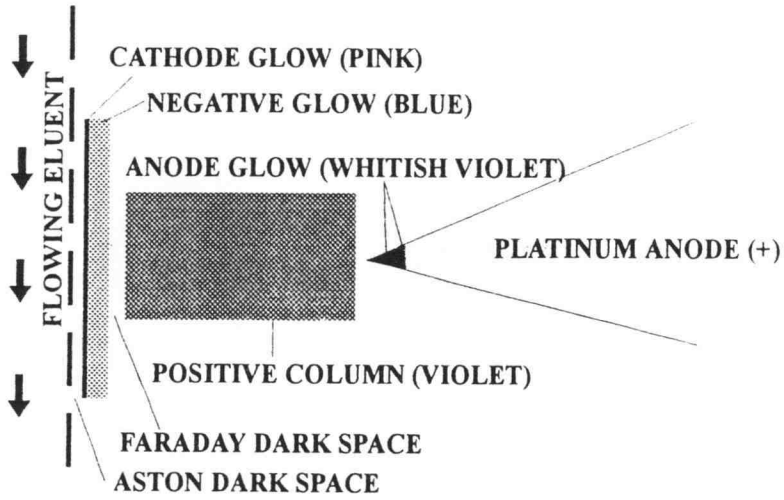

OSCILLATING GLOW DISCHARGE

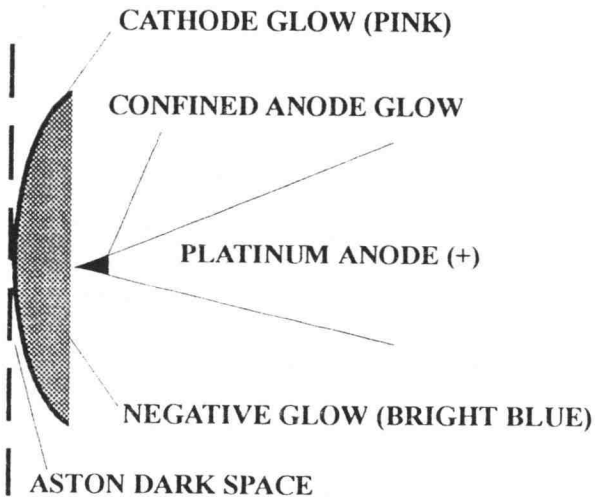

Figure 2.4. Appearance of the nonoscillating and oscillating glow discharge at a magnification factor of approximately 50x.

surface of the solution, with a thickness of 0.01 mm. Cathode glow areas ranging from 2×10^{-4} to 7×10^{-4} cm^2 have been observed for currents of 0.2 and 0.8 mA, respectively yielding a relatively constant current density (current / cathode glow area) of 1100 mA/cm^2. The glow discharge seems to mimic the constant current density behavior of a normal glow discharge.[10] As current is increased, the diameter of the cathode glow increases to keep the current density approximately constant. The thickness of the negative glow region also remains approximately constant with increase in current, agreeing with normal glow discharge behavior.[11]

The cathode glow appears to float on a dark region, the Aston dark space, which is in direct contact with the solution. The thickness of the dark space is 0.02 mm. The cathode glow is immediately followed by a bluish negative glow 0.02 mm thick. The negative glow appears to be significantly less intense than the cathode glow, contrary to the intense luminosity of the negative glow in a glow discharge under reduced pressure. The negative glow is followed by the Faraday dark space, with a thickness of 0.02 mm, which is, at electrode distances greater than 0.05 cm, immediately followed by a uniform whitish violet positive column. The positive column is cylindrical in shape, and its length increases with electrode spacing. The diffuse whitish anode glow follows the positive column and is most intense at the anode tip but gradually fades up the side of the anode.

Similar to a conventional glow discharge, as anode distance is decreased the positive column length decreases,[10] with no change in the regions near the cathode until the anode enters the Faraday dark space. It is not possible to reduce the electrode distance enough to cause the negative glow to disappear, because eluent tends to surge towards the anode and extinguish the discharge at electrode distances less than 8 μm.

2.4.4 Discharge Behavior at Distances Below 0.01 cm

Figure 2.4 shows the appearance of the glow discharge at electrode distances below approximately 0.01 cm. In general, when the electrode distance is decreased below this value, the appearance of the glow discharge changes dramatically, and stable high frequency (13-25 MHz) oscillations are observed. The negative glow forms a bluish spherical segment tangent to the flowing solution, with a very thin pinkish cathode layer evenly distributed on the surface of the segment. The negative glow fills the spherical segment in much the same way the negative glow fills a traditional metallic hollow cathode. The spherical segment has a constant altitude of 0.021 mm and diameter of 0.13 mm, yielding a lateral area of 1.5×10^{-4} cm^2. The cathode glow is much less intense than the negative glow and sometimes appears to be completely absent. The spherical segment floats on the Aston dark space, and the liquid flow is tangent to the midpoint of the rim of the spherical

segment, where the dark space thickness is at a minimum. This thickness is below the 0.004-mm resolution of the measuring device. Visible reflections of the spherical segment in the liquid surface indicate that the segment is not an indentation in the liquid surface and that the liquid surface remains flat.

The Faraday dark space, extending 0.02 mm from the negative glow dish, is immediately followed by the anode glow, which is neatly confined over a 0.02-mm length of the anode tip. The anode glow does not diffuse up the anode tip as it does with larger electrode spacings but rather appears as a very bright, well defined glowing region on the tip of the anode.

If the anode glow loses its unique confinement during adjustments, the spherical segment immediately reverts to the flat disc shape discussed earlier and the oscillations disappear. The electrode spacing boundary between the non-oscillating flat disc discharge and the oscillating spherical segment discharge with a confined anode glow is at the edge of the Faraday dark space, where the positive column starts to form. As soon as the positive column starts to form, as the electrode spacing increases, the anode glow confinement is lost, and the spherical segment shape disappears. Thus it appears that oscillations are dependent on either the uniquely confined anode glow or the spherical segment shape of the discharge or both.

The anode glow confinement is dependent upon the angle of inclination of the anode. In general, it has been observed that the greater the angle of inclination of the anode tip, the more difficult it is to achieve anode glow confinement. As the angle of inclination increases, eluent surging is more likely to extinguish the glow discharge because larger angles of inclination move more electrode area nearer the liquid. It has been found that an angle of inclination of 15° provides anode glow confinement and minimal tendency for the eluent to surge.

The cathode current density behavior of the spherical segment glow discharge discussed above approximates the behavior of an abnormal glow discharge.[10] An increase in current results in a proportional increase in current density, with no measurable change in the lateral area of the spherical segment. Current densities ranging from 1000 to 7000 mA/cm^2 have been observed. If the current is increased much above 1 mA, the anode confinement is lost, and the discharge reverts to the flat disk shape, with normal glow discharge behavior resuming without oscillations. Higher currents also tend to increase eluent surging.

2.4.5 Discharge Oscillations using a Liquid Cathode

Glow discharge oscillations for the liquid cathode occur with electrode spacings below 0.01 cm when the negative glow assumes a spherical segment shape.

Frequencies ranging from 7 to 25 MHz (250 mV peak to peak) have been observed, depending on electrode distance, anode shape, electrolyte concentration, electrolyte type, current, and cell voltage. The oscillation waveform, as monitored from the sampling resistor, resembles a sine wave and is often not perfectly symmetrical but has the appearance of a large amplitude primary oscillation combined with a smaller amplitude higher frequency secondary oscillation. A symmetric waveform is obtained when the anode is exactly perpendicular to the liquid surface and when the anode tip has close to perfect symmetry. Such an exact arrangement is difficult to produce and most waveforms observed are slightly asymmetric.

Lower frequency oscillations around 1 MHz have been observed at electrode spacings of approximately 1 cm. However, the noise is usually high, and the analyte signal is very low. It is speculated that these oscillations occur in the positive column, and the low response in frequency to an analyte injection substantiates this, because it is known that processes in the cathode region of a glow discharge have little or no effect on the positive column as long as the positive column is continually supplied with electrons.[11]

Frequency noise is caused by a variety of factors. Mechanical vibration seems to contribute most significantly to the noise, and most of this is eliminated by the vibration-dampening intertubes. Electrolyte concentration

also influences noise, and it has been found that as electrolyte concentration increases, noise decreases. On the other hand, as electrolyte concentration increases, the range of oscillation frequencies available, as determined by changing the electrode spacing, decreases.

In general, oscillations do not occur until the sodium chloride concentration is approximately 30 μg/mL. Below this value, the spherical segment shape does not form and no oscillations are present. With a sodium chloride concentration in the range of 30-85 μg/mL, oscillations exist over a wide frequency range (7-20 MHz) but tend to have significant noise (typically 40% of frequency value). At a concentration of approximately 90 μg/mL NaCl, the noise suddenly decreases. As the electrolyte concentration is increased further, the noise decreases slightly, but at the expense of a decrease in the current and frequency analyte signals. This behavior is quite similar to a conductivity detector, where the response decreases with higher background electrolyte levels. There appears to be an optimal electrolyte concentration of 90 μg/ml NaCl that yields the highest signal-to-noise ratio.

2.4.6 Potassium Nitrate Injections

Figure 2.5 shows the simultaneous frequency and current responses of nine 78 μg/mL KNO_3 injections in a mobile phase of 90 μg/mL NaCl. The large vertical noise spikes correspond to valve switching times. The mass injected is

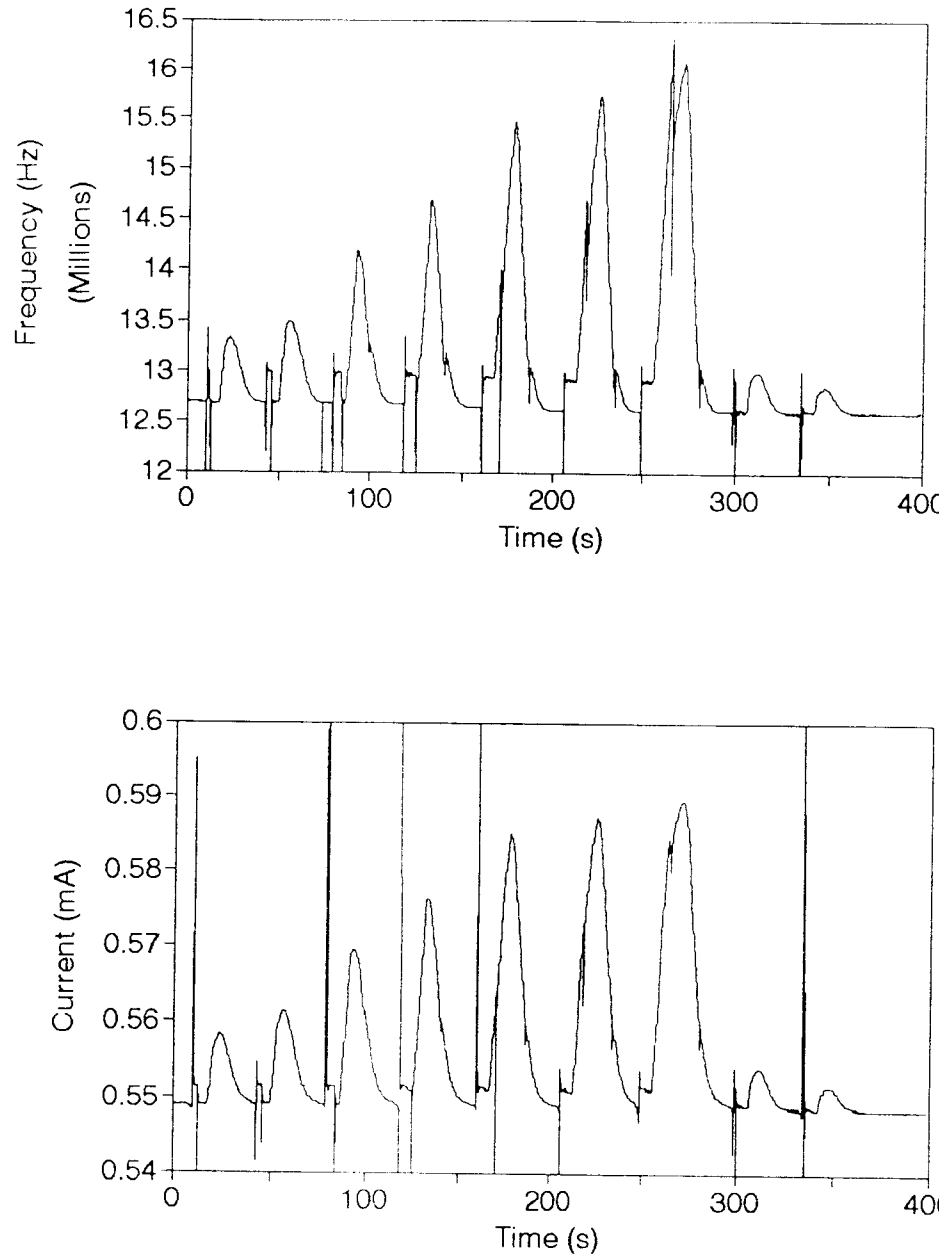

Figure 2.5. Simultaneous frequency and current responses to a series of potassium nitrate injections described in the text.

proportional to the duration of the injection. The duration of each injection is indicated by the spacing between these transient signals, the second of which occurs during the peak when the peak is large. The mass of KNO_3 corresponding to each peak, is 1.2, 1.6, 2.7, 3.8, 5.7, 6.7, 8.7, 0.80, and 0.54 μg, respectively. The average baseline frequency and current, as determined from averaging 50 points of the baseline, are 12 598 000 Hz and 0.545 mA, respectively. The cell voltage is -340 V, and argon flow rate is 0.25 mL/min. The negative glow of the glow discharge has a spherical segment shape, with an approximate electrode distance of 10 μm.

The standard deviations in the frequency and current as determined from 50 points of the baseline are 2000 Hz and 3.0×10^{-5} mA, respectively. The response ratio (peak height/average baseline) for the frequency and current is approximately the same for all peaks with a similar signal-to-noise ratio for the current and frequency, respectively.

Figure 2.6 shows the oscillation-frequency and current calibration curves for these nine injections. When the injection time is much less than the peak width, the area or height of the peak should be proportional to the amount injected. Linearity is lost beyond 2 or 3 μg, because the response eventually limits at the concentration of the analyte reservoir. Dividing the noise (3 times the standard deviation, 3SD) in the frequency and current by the slope of the line through the first five points shows that an

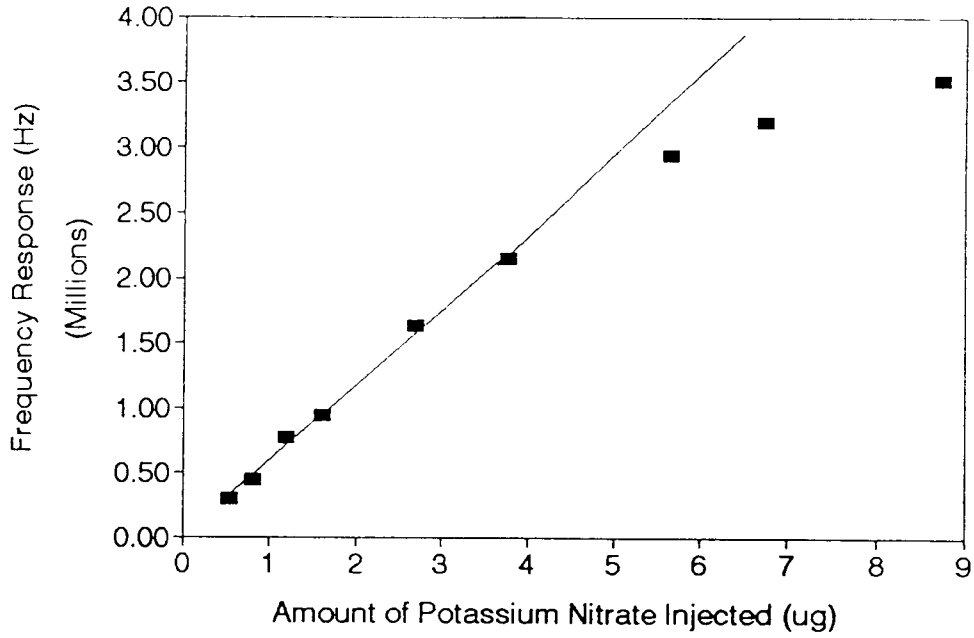

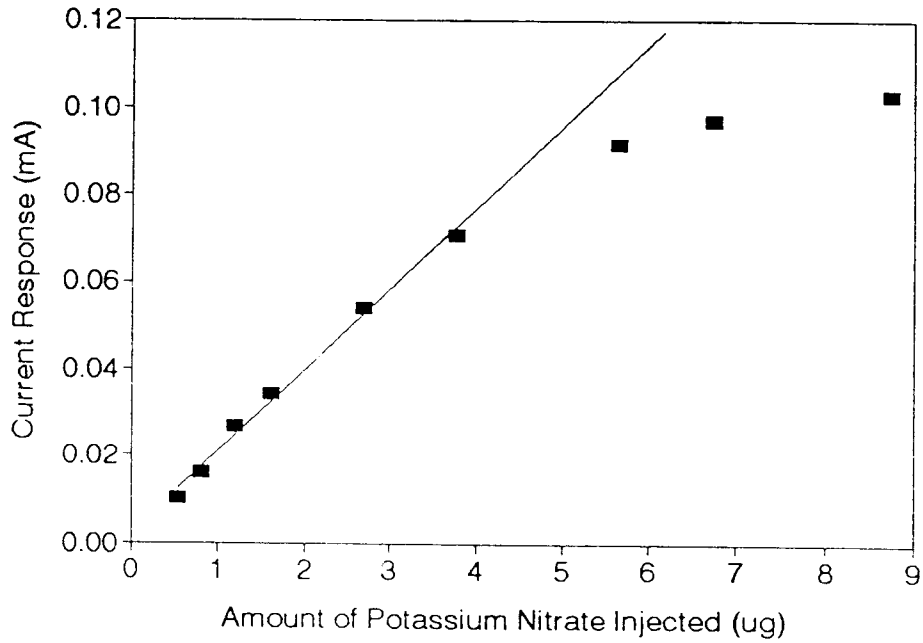

Figure 2.6. Potassium nitrate calibration curves for frequency and current responses as desribed in the text.

injection of 8 ng (80 pmol) yields a signal equal to 3SD of both the frequency and current baselines. Using the 0.4 μL detector cell volume and the peak volume at half height of the smallest peak (77 μL) yields in-cell mass and concentration detection limits of approximately 600 fmol and 2 μM potassium nitrate, respectively.

2.4.7 Sucrose Injections

Figure 2.7 shows the frequency and current response of a 3.8-s injection of 160 μg/mL sucrose solution, causing 4.3 μg of sucrose to pass through the detector. The frequency and current peak volume as measured from the peak width at half height is 90 μL. The cell voltage was 317 V, and argon flow rate 250 mL/min. Average baseline oscillation frequency and current values, obtained by averaging 25 points of the baseline, are 11 365 000 Hz and 0.481 mA, with standard deviations of 1000 Hz and 8.1 x 10^{-6} mA, respectively. The relative frequency and current responses (peak height / baseline) are approximately the same, and each has a similar signal-to-noise ratio. An injection of 75 ng (219 pmol) of sucrose yields a signal equal to 3SD of the baseline for frequency and current, resulting in in-cell mass and concentration detection limits of approximately 1 pmol and 3 μM sucrose, respectively. Sucrose was used to demonstrate the detector response to a nonconducting, nonvolatile organic species.

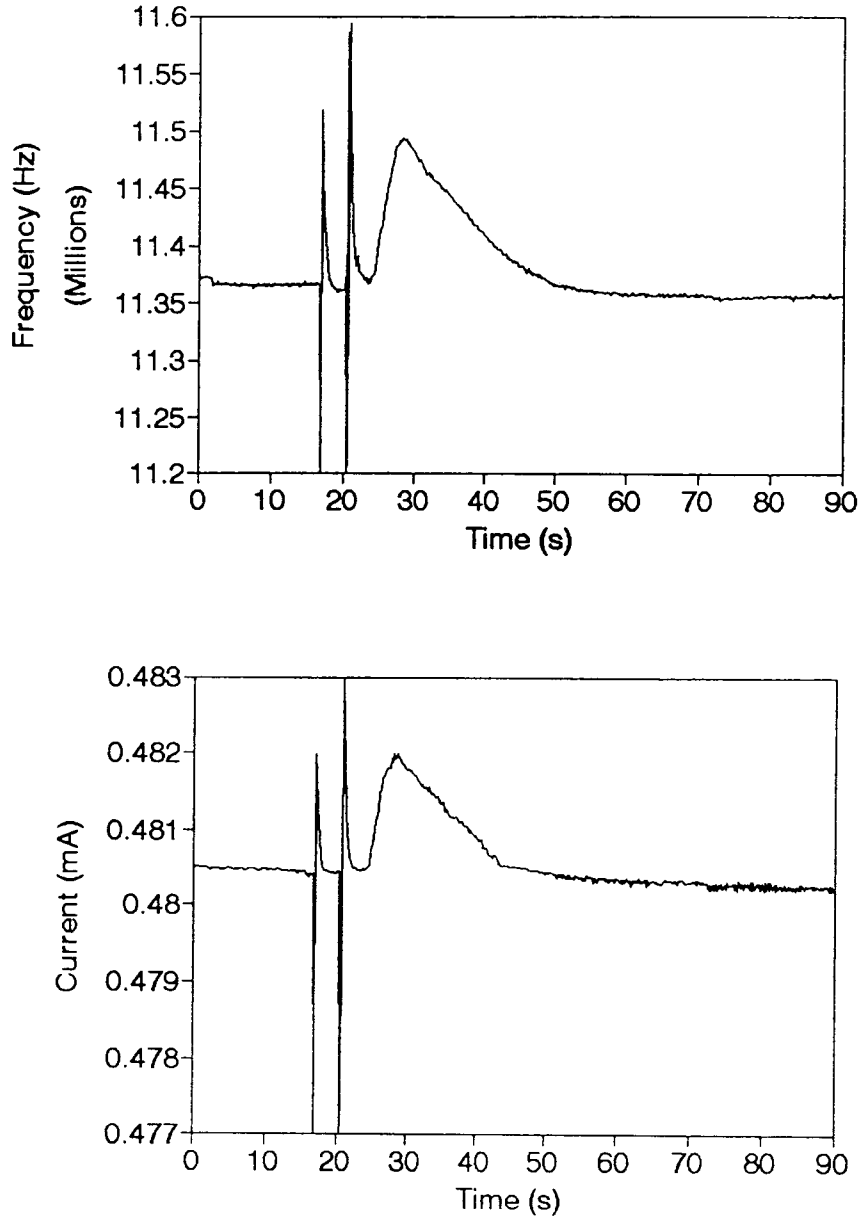

Figure 2.7. Simultaneous frequency and current responses to a 4.3-μg sucrose injection as described in the text.

2.4.8 Current Response Mechanism

The mechanism of current response to analyte impurity in a liquid-interfaced glow discharge has not yet been established. It could be speculated for an electrolytic species (such as KNO_3) that the passing of a conducting analyte zone between the electrodes causes a relative increase in solution conductivity and thus an increase in the current passing between the electrodes. Experimental data for KNO_3 shows that the calculated conductance ratio ($\Delta G_a/\Delta G_b$) for two different KNO_3 masses in aqueous NaCl solution is similar to the ratio of their current peak responses ($\Delta I_a/\Delta I_b$). Also the ratio of the absolute (total) values of conductance is the same as the ratio of the total currents.

No simple explanation for the current response can be found when a nonconducting analyte zone (such as sucrose) passes between the electrodes. A decrease in conductivity and current would be expected, contrary to the experimental results for sucrose. One possible explanation is that sucrose undergoes oxidation and decomposition from the high energy ions produced in the glow discharge that strike the solution surface, yielding products which increase the conductivity of the solution. While irradiated sucrose solutions have not been studied in great detail, the oxidation and decomposition scheme is thought to resemble that of an irradiated glucose solution in which yields of gluconic acid, glucuronic acids, hydrogen, carbon dioxide,

and carbon monoxide are formed.[12] Any gases released from the solution could also affect the potential of the cathode fall, which would result in a change in current. It has been found that even trace amounts of some gases cause large changes in the value of the cathode fall of a glow discharge.[13]

2.4.9 Frequency Response Mechanism

A possible explanation for the frequency response is the change in surface tension of the solution due to the passing analyte zone. The change in surface tension might change the position of the liquid surface, causing a change in electrode spacing. We have found that oscillation frequency is very sensitive to changes in electrode distance, and in general, as electrode distance increases, the frequency decreases relatively more rapidly than current. Since the frequency and current both increase by the same factor for sucrose and KNO_3 injections, a change in surface position does not seem to be a major cause of the analytical signal.

The relationship between the current and frequency responses in a glow discharge detector is not yet known. Recent studies using a glow discharge detector for gas chromatography reveal very complex relationships.[14] In those studies, the frequency and current responses could be in the same or opposite directions, depending upon plasma conditions. The relative frequency and current responses in

this study are approximately equal whether the analyte is electrolytic or nonelectrolytic. This could suggest that, in our case, the frequency and current responses are influenced by the same mechanisms.

2.5 Conclusions

It has been shown that the liquid-interfaced oscillating glow discharge detector is able to detect trace quantities of an inorganic and nonelectrolytic organic compound in a flowing aqueous solution of 90 μg/ml NaCl. The ability to detect femtomole quantities of analyte within a 400-nL detector volume makes it a potentially useful detector for other aqueous flowing systems, such as capillary electrophoresis and liquid chromatography. Future studies will reveal whether or not the eluents used in these techniques are able to support the establishment of the oscillating glow discharge.

The analysis of carbohydrates is receiving increasing attention, and several authors report precolumn derivatization counterelectroosmotic capillary electrophoresis with direct UV detection as the most sensitive method available for carbohydrate analysis, with a mass and concentration detection limit as low as 1 fmol and 1 μM, respectively for glucose.[15] The oscillating glow discharge detector, with in-cell concentration and mass sucrose detection limits of 3 μM and 1 pmol, respectively

exhibits a similar concentration sensitivity. The 2 μM frequency and current detection limits observed for potassium nitrate using a glow discharge detector are also comparable to those of currently available capillary electrophoresis and liquid chromatography conductivity detectors, which typically detect in the 10-0.1 μM range.[15,16] Therefore, although our study focuses only on the detection of two analytes and the eluent differs from the buffers and mobile phases typically used in capillary electrophoresis and liquid chromatography, it appears worthwhile to test modified versions of the new detector on such systems.

Future studies will focus on the current and frequency responses of other organic compounds. It has been found previously that the frequency and current responses of a low pressure glow discharge detector for gas chromatography vary for different compounds.[14] It is hoped that the liquid-interfaced oscillating glow discharge detector will provide similar qualitative as well as quantitative information for flowing liquid systems.

2.6 Acknowledgment

The financial support of the National Science Foundation (Grant CHE-9013929) and the National Institute of Health (Grant ES00210 from NIEHS) is gratefully acknowledged.

2.7 References

[1] Bockris, J.O.; Conway, B.E.; Hickling, A. *Modern Aspects of Electrochemistry*, No.6, Plenum Press: New York, 1971, 329-404.

[2] Hickling, A.; Ingram, M.D. *J. Electroanal. Chem.* 1964, 8, 65-81.

[3] Hickling, A.; Denaro, A.R. *J. Electrochem. Soc.* 1958, 105, 265-270.

[4] Hickling, A.; Davies, R.A. *J. Chem. Soc.* 1952, 3595-3602.

[5] Hickling, A.; Linacre, J.K. *J. Chem. Soc.* 1954, 711-720.

[6] Cserfalvi, T.; Mezei, P.J. *Anal. At. Spectrom.* 1994, 9, 345-349.

[7] Petrovic, Z.Lj.; Phelps, A.V. *Amer. Phys. Soc.* 1993, 47, 2806-2822.

[8] Donahue, T.; Dieke, G.H. *Phys. Rev.* 1951, 81, 248-261.

[9] Piepmeier, E.H.; Cook, B. *Anal. Chem.* 1991, 63, 1763-1766.

[10] Nasser, E. *Fundamentals of Gaseous Ionization and Plasma Electronics*; Wiley-Interscience: New York, 1971.

[11] Penning, F.M. *Electrical Discharges In Gases*, Macmillon Co.: New York, 1957.

[12] Allen, A.O. *The Radiation Chemistry of Water and Aqueous Solutions*; Van Nostrand: New York, 1961.

[13] Maxfield, F.A.; Benedict, R.R. *The Theory of Gaseous Conduction and Electronics*, McGraw-Hill: New York, 1941.

[14] Smith D.L.; Piepmeier, E.H. *Anal. Chem.* 1994, 66, 1323-1329.

[15] Jandik P.; Bonn, G. *Capillary Electrophoresis of Small Molecules and Ions*; VCH Publishers: New York, 1993.

[16] Miller, J.M. *Chromatography: Concepts and Contrasts*; John Wiley & Sons: New York, 1988.

Chapter 3

A New, Sensitive Glow Discharge-Conductivity Detector For Carbohydrates In Aqueous Chromatography

Christopher J. Herring and Edward H. Piepmeier

Submitted to *Analytical Chemistry*
(July, 1996, in press)

3.1 Abstract

Recently, there has been increasing interest in the analysis of carbohydrates attached to glycoproteins. Since the initial amount of glycoprotein is typically very low the use of a very sensitive carbohydrate detector is critical to the analysis. In this paper a new glow discharge-conductivity detector is shown to respond to low nanomolar and femtomole quantities of carbohydrates in aqueous high performance liquid chromatography. Its sensitivity is comparable to the most sensitive detection methods available for carbohydrate analysis. The atmospheric pressure argon glow discharge is sustained between two metallic electrodes and is operated near the flowing eluent output of a liquid chromatography system. The glow discharge induces oxidation in the eluting carbohydrates, forming acid in amounts proportional to carbohydrate concentration. The relative acid concentration is monitored with a conductivity detector placed downstream from the discharge region. A detailed description of the detector and the parameters that control sensitivity are presented. The formation of hydrogen peroxide, acid, and UV absorbing species in aqueous glucose solutions are also studied using both liquid-interfaced and non-liquid-interfaced glow discharge configurations. A comparison between these products and the products formed under similar conditions using high energy radiation is presented.

3.2 Introduction

Carbohydrates are a class of compounds which have numerous biologically significant roles. They are important in the structural development of cells, metabolism, immunity, energy storage, blood clotting, and in a variety of other biological processes. There is increasing interest in the analysis of carbohydrate moieties cleaved from glycoproteins. Glycoproteins have very specific biological functions and it is believed that the structure of each carbohydrate determines the function of the glycoprotein.[1,2] Such analyses require the use of high resolution separation techniques such as high performance liquid chromatography[3,4] (HPLC) and capillary electrophoresis (CE).[5] A common hinderance is that the initial amount of glycoprotein is often very small and requires the use of a very sensitive detector. Thus the development of highly sensitive detectors for carbohydrate analysis is critical to the study of carbohydrates and glycoprotein function.

A major problem with carbohydrate detection in liquid chromatography is that most carbohydrates lack chromophores and fluorophores, thus limiting the use of UV and fluorescence detectors. There has been some success in detecting carbohydrates at low wavelengths[6] (180-200 nm) but detection limits are poor due to low molar absorptivities. There have been numerous cases[7] where carbohydrates were derivatized to produce UV absorbing or fluorescing

compounds, yielding detection limits in the picomole range. While the sensitivities of derivatization techniques are high, the instrumentation and procedures tend to complicate the analysis.

Differential refractive index detection is currently the most common detector used for carbohydrate analysis, and responds universally to all carbohydrates. It suffers, however, from poor sensitivity, a limited linear range, and an incompatibility with gradient elution which is often required for oligosaccharide separations.

The most sensitive detector for carbohydrate analysis is the pulsed amperometric detector which is typically used in conjunction with high performance anion exchange chromatography. A highly alkaline aqueous mobile phase (pH > 11) is typically used to obtain optimal sensitivity and efficiency. Concentration and mass detection limits are in the low nanomolar and picogram regions, respectively. Disadvantages include the need for a very high mobile phase pH and a reduction in sensitivity for higher molecular weight oligosaccharides.

The evaporative light scattering detector is another increasingly popular carbohydrate detector. This detector responds universally to all carbohydrates and can be used with gradients. It suffers, however, from high detection limits[8] and some compatibility problems[6] with aqueous mobile phases.

In general there still exists the need for a simple, inexpensive, highly sensitive and universal carbohydrate detector. This paper describes the development of such a detector for aqueous liquid chromatography. In a previous paper[9] it was shown that an aqueous liquid-interfaced glow discharge could be used as a detector for sucrose in a flow injection system by monitoring the change in glow discharge current and oscillation frequency. Concentration and mass detection limits were 3 μM and 1 pmol, respectively. It was speculated that the response was due to the formation of an acid induced by the oxidative nature of the glow discharge.

Glow discharge induced transformations in aqueous solutions have been the subject of much study. Several authors[10-12] have shown that a glow discharge sustained between a metallic anode and aqueous cathode (glow discharge electrolysis) oxidizes solution species in excess of that predicted by Faraday's law. The oxidation of aqueous Fe^{2+} has been found to reach 8 mol/Faraday when the solution is made the cathode of a glow discharge, and this is vastly in excess of the 1 mol/Faraday predicted from Faraday's law. It has been established that this excess oxidation is due to the presence of oxidizing hydroxyl radicals which are generated in solution by water dissociation caused by the impacting H_2O^+ ions.[10-14] While there have been numerous studies on the glow discharge induced oxidation of various aqueous inorganic species, there have been few on the transformations induced in aqueous organic solutions.[11,15-17]

The similarities between the products formed in aqueous solutions irradiated with high energy radiation and solutions interfaced to a glow discharge are well established. In general, aqueous solutions exposed to high energy radiation yield hydrogen peroxide, hydronium ions, hydrogen, hydrated electrons, and the OH and H radicals.[18] Among these, only hydrogen peroxide, hydrogen, and hydronium ions are stable solution products. The formation of these stable products is linked to reactions between transient radiolysis products. For example, the dimerization of OH and H radicals leads to hydrogen peroxide and hydrogen, respectively. The production of hydrogen peroxide and hydrogen in glow discharge electrolysis has been thoroughly investigated, but no studies on the formation of hydronium ions have been made. Many authors have concluded that the glow discharge induced solution mechanisms leading to these products are the same as the high energy radiation induced solution mechanisms.

To date there have been no studies investigating the glow discharge induced transformation of aqueous carbohydrate solutions. There have been, however, numerous studies on the radiation induced decomposition of aqueous carbohydrates.[18-22] The decomposition of carbohydrates has been shown to be primarily due to hydroxyl radicals, formed from the decomposition of water. Hydroxyl radicals react rapidly with carbohydrates forming carbohydrate radicals which undergo various complex reactions leading to a large

number of products. For example, when aqueous glucose is irradiated with gamma-ray or X-ray radiation, 25 to 30 stable products are formed.[18] Irradiation of aqueous solutions of monosaccharides, disaccharides, polysaccharides, and oligosaccharides all form similar types of compounds including deoxy-compounds, deoxyketo-compounds, and various acids. Many of these products are formed in amounts proportional to radiation dose and their concentrations generally increase with increasing carbohydrate concentration. The products most commonly monitored after the irradiation of aqueous carbohydrates are malonic dialdehyde, acid, and hydrogen peroxide. Malonic dialdehyde absorbs strongly at 260 nm ($\epsilon \sim 2 \times 10^4$ L mol^{-1} cm^{-1}) and is monitored using UV spectrometry. Acid and hydrogen peroxide are conveniently monitored by pH and spectrophotometric methods[23], respectively.

This paper reveals for the first time the similarities between the products formed in aqueous carbohydrate solutions exposed to a glow discharge and to high energy radiation. It is shown that the same products are formed whether the glow discharge is interfaced directly to the solution or operated between metallic electrodes near the solution. Finally, it is shown how monitoring the relative acid concentration, formed by the glow discharge, results in a new, highly-sensitive carbohydrate detector for aqueous liquid chromatography.

3.3 Experimental

3.3.1 Glow Discharge Conductivity Detector Interface

Figure 3.1 shows the main components of the detector interface with the outer brass cell removed. Figure 3.2 shows top and side views of the outer brass cell containing the components shown in figure 3.1 and has been described previously.[9] Liquid enters the cell through 1/16-in.-o.d. x 0.010-in.-i.d. PEEK tubing (poly(ether ether ketone)), flows down a 3- x 60- x 0.5 mm microscope slide cover, over a platinum wire electrode, and out a 1/32-in. hole in the steel baseplate. In order to prevent pulsations from liquid dripping off the baseplate, the liquid flows smoothly down a standard microscope slide supported in a 250 ml beaker. The platinum wire electrode (2-in. x 1/64-in.-diameter), inserted through the tygon tubing, touches the glass slide 0.2 cm above the steel support clamp electrode, and forms a detector solution volume of approximately 10 μL. The platinum wire is connected to a function generator (Tektronix, TM501) which provides a 1-kHz, 4 V signal. The steel base is connected to the conductivity detector circuit as described later.

The glow discharge operates between two identical brass electrodes. Each electrode consists of a tapered 1/16-in. diameter x 0.2-in.-length brass rod pushed 0.2-cm into a 1/8-in.-o.d. x 1/16-in.-i.d. x 6-in.-length stainless steel tube. Argon (99.99%, 100 ml/min) enters the cell through

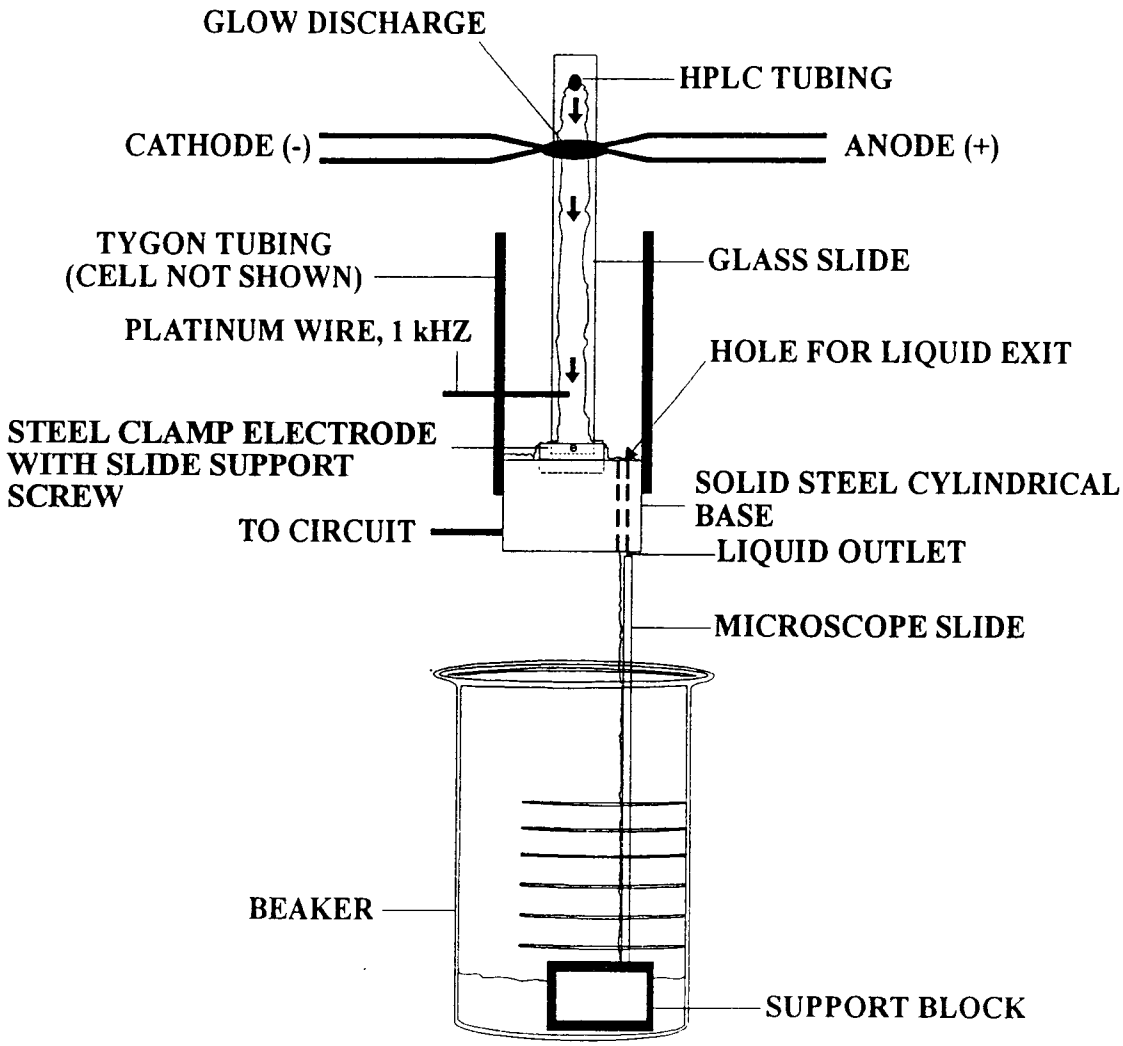

Figure 3.1. Schematic diagram of the glow discharge-conductivity detector interface. Not to scale.

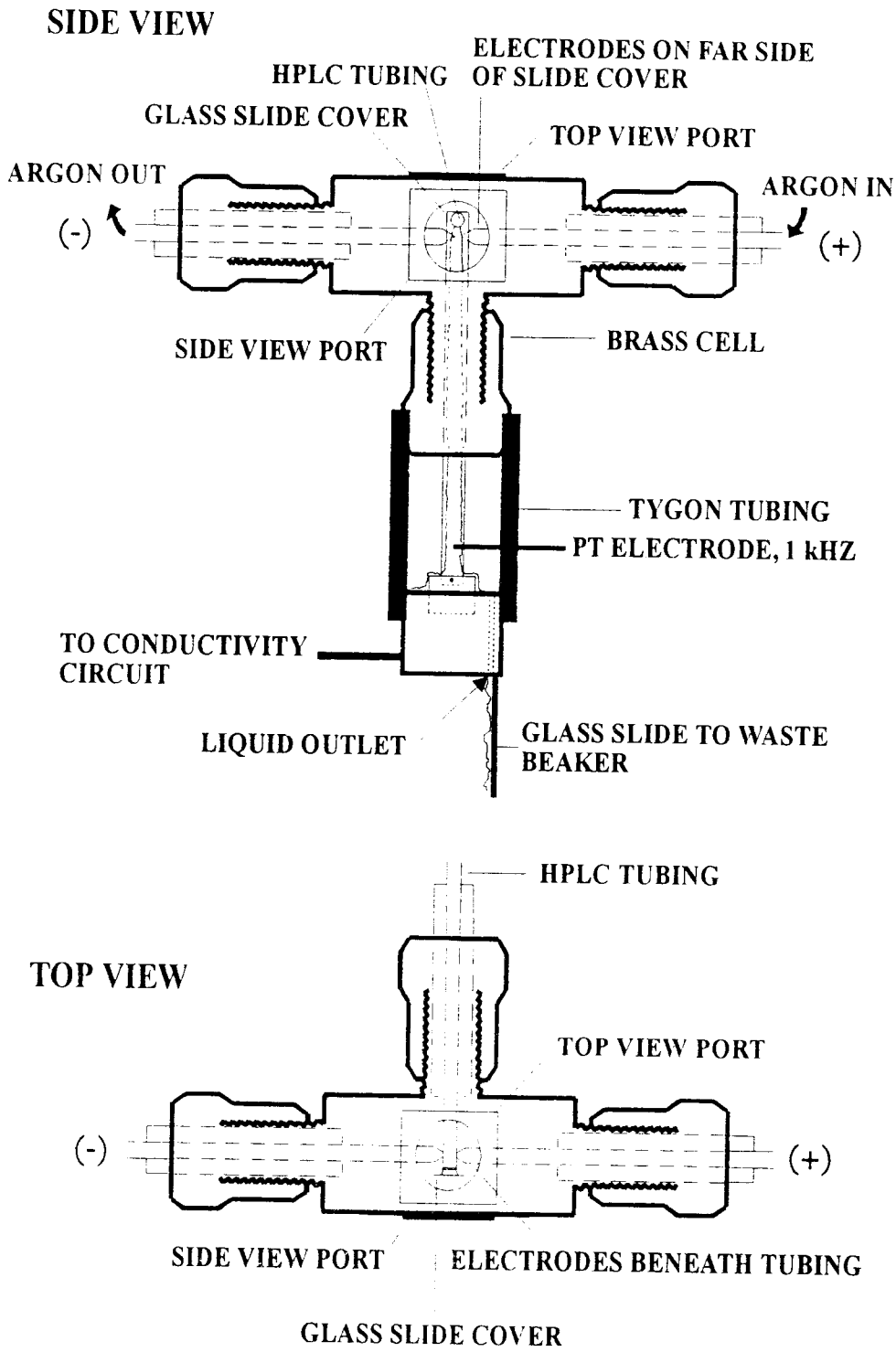

Figure 3.2. Schematic diagram of the external brass cell containing the glow discharge in figure 1.

the anode and exits via the cathode in a manner described previously.[9] In this way the glow discharge is isolated from the atmosphere and only argon is present in the cell. Argon is supplied to the anode through a 2-meter length of 1/4-in.-o.d. x 1/8-in.-i.d. Teflon tubing attached to the output of a mass flow meter (Tylan, model 20A). The mass flow meter connects to a regulated argon supply through a 4-meter length of similar sized copper tubing.

3.3.2 HPLC Setup

A diagram of the chromatography setup is shown in figure 3.3. An HPLC pump (Eldex, model AA) pumps the mobile phase from a stoppered 1-L flask through two 80-cm lengths of 1/8-in.-o.d. x 1/16-in.-i.d. Teflon tubing. Mobile phase filters (Alltech, 2 μm) are connected to the Teflon tubes in the mobile phase reservoir. A sparging tube also protrudes through the flask stopper and is connected to a regulated helium tank (99.99 %) through 2 m of 1/8-in.-o.d. x 1/16-in.-i.d. Teflon tubing. All mobile phases where filtered through 0.2-μm filter paper (Rainin, Nylon-66) and degassed for 10 min before use.

Two 50-cm lengths of 1/16-in.-o.d. x 0.020-in.-i.d. steel tubing each connect to one of the two pump outputs and are joined via a steel tee (Valco, 1/16-in. x 0.25-mm). Another 50-cm length of steel tubing connects the tee to the input of a pulse dampener (SSI LO-pulse, Alltech). The pulse dampener output connects through a 50-cm length of

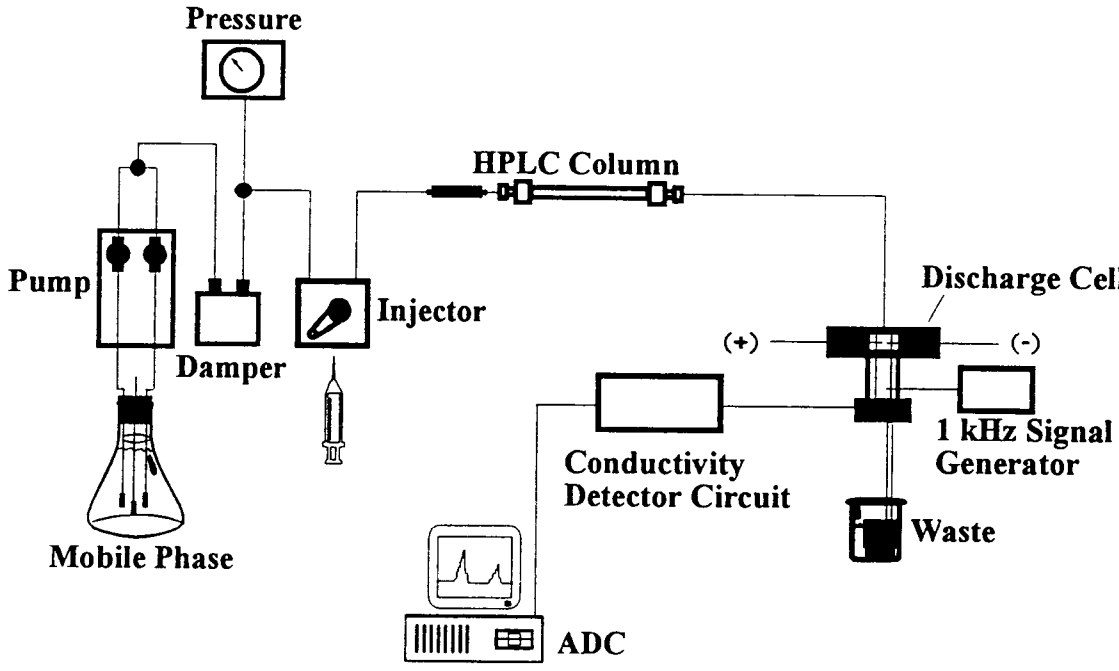

Figure 3.3. Schematic diagram of the high performance liquid chromatography setup.

steel tubing to another tee which connects to a pressure gauge (Alltech, 0-5000 psig). The tee also connects through a 70-cm length of 1/16-in.-o.d. x 0.010-in i.d. PEEK tubing to a 6-way high pressure injection valve (Alltech, model 9010). The injection valve is used with 6- or 20-μL injection loop volumes and is configured for manual injection. Injections are made with a 10-ml polyethylene syringe equipped with a disposable filter (0.2-μm, Nylon). For all injections the loop is washed with several volumes of doubly deionized water and then the sample. An injection consists of manually switching the valve to the inject position and leaving it there for the duration of the run. The injection valve is connected to a guard column (Alltech Econosphere, C-18, 30- x 4.6-mm, 5 μm) and separation column (Alltech Econosphere, C-18, 250- x 4.6-mm, 5 μm) with 8 cm of PEEK tubing. A 1-meter length of PEEK tubing connects the column outlet to the glow discharge-conductivity detector. Before use the system is purged with mobile phase at 1 ml/min for 15 min.

3.3.3 Glow Discharge Circuit and Operating Conditions

The circuit used to generate the atmospheric pressure argon glow discharge is shown in figure 3.4. The discharge is powered by a high voltage power supply (Hewlett Packard, 6516A, 0-3000 V) set to +1600 V. Discharge current is controlled by adjusting a variable resistor. Unless

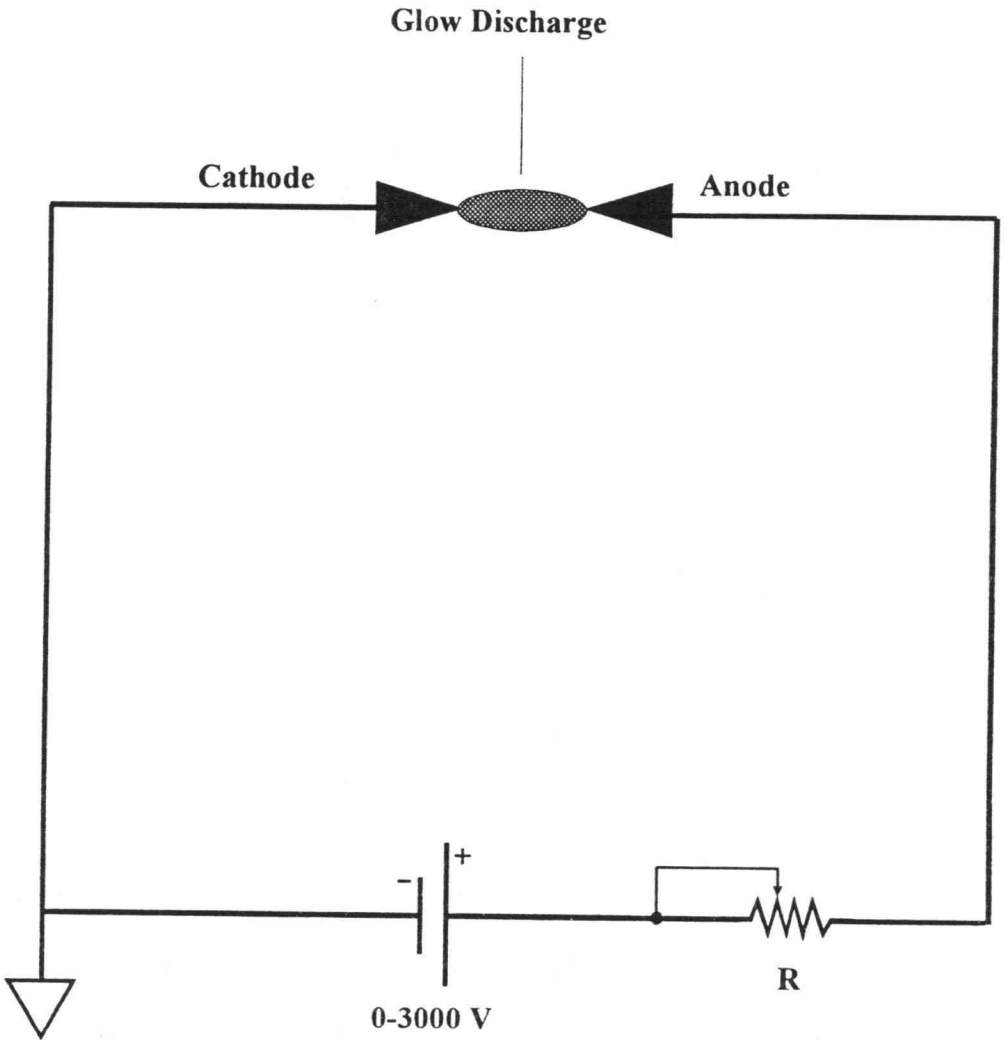

Figure 3.4. Diagram of the circuit used to form any glow discharge.

otherwise stated, the discharge is operated with current and cell voltages of 2 mA and 200 V, respectively.

3.3.4 Conductivity Detector Circuit

The conductivity detector circuit is shown in figure 3.5 and is based on a circuit designed by Ahmon.[24] The circuit is built on a PowerAce (model 203) breadboard and is surrounded by a 37- x 28- x 16-cm copper plate Faraday cage. All op-amps are TL081CP JFET-input amplifiers (Texas Instruments) because of their low cost, high input impedance, and low input bias current.

A 1-kHz signal provided by the function generator is sent to the flowing solution (R_s in figure 3.5) through the platinum electrode. The steel base electrode is connected by a 10-cm length of 22-gauge circuit board wire to the inverting input of operational amplifier (A). R_s is approximately 23 MΩ for an aqueous non-conducting mobile phase. For solutions containing an electrolyte, R_f is reduced to prevent op-amp saturation. The output of amplifier (A) is fed through a high pass filter with gain (B) eliminating any DC offset from the glow discharge. This signal is sent to amplifiers (C) and (D), which function as a precision full-wave rectifier, then to a low pass filter (E) with time constant 0.02 s. The DC output is then fed to a DASH-8 (Metrabyte) ADC located inside a computer, and is monitored with a program developed previously.[9] The above configuration is easily constructed, inexpensive, and

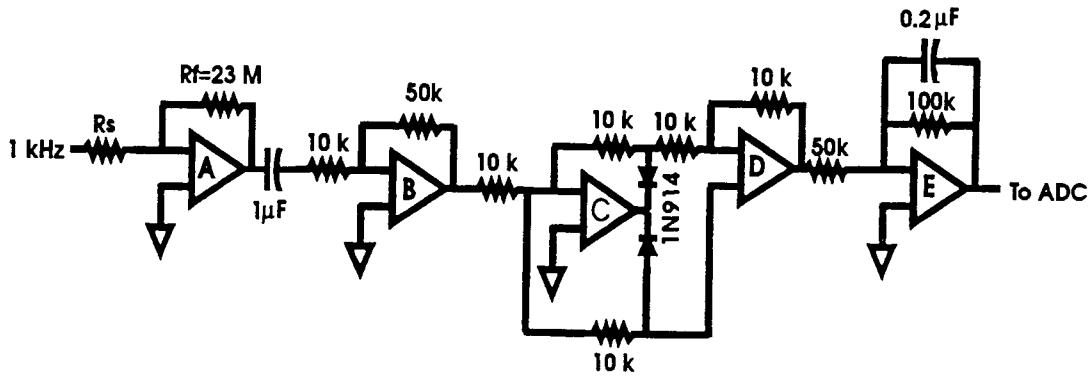

Figure 3.5. Schematic diagram of the conductivity detector circuit.

yields a DC output directly proportional to the conductance of the flowing solution.

3.3.5 Liquid Electrode Setup

Figure 3.6 shows the apparatus used in auxiliary experiments to expose aqueous solutions to an atmospheric pressure glow discharge operating between a metallic and liquid electrode. A 180-ml beaker is used as the glow discharge cell / solution chamber and is sealed from the atmosphere with a rubber stopper through which two electrodes protrude. The liquid electrode is formed by submerging a 1/64-in diameter coiled platinum wire soldered to a 5-in length of 1/8-in.-o.d. x 1/16-in.-i.d. steel tubing. The discharge occurs between the pointed brass electrode (described earlier) and liquid surface. Argon flows through the anode at 100 ml/min and exits the cathode. The anode is located 0.5 cm above the solution and the discharge is initiated by applying a 50,000 V tesla coil pulse to the anode. Discharge current is held constant (± 0.1 mA) by adjusting the current limiting resistor. Unless otherwise noted the discharge current is kept at 2.0 ± 0.1 mA. In each case the volume of solution analyzed is 25.0 ml and exposure times are measured using a stop watch. Irradiated samples are stored in 30-ml glass vials until ready for analysis.

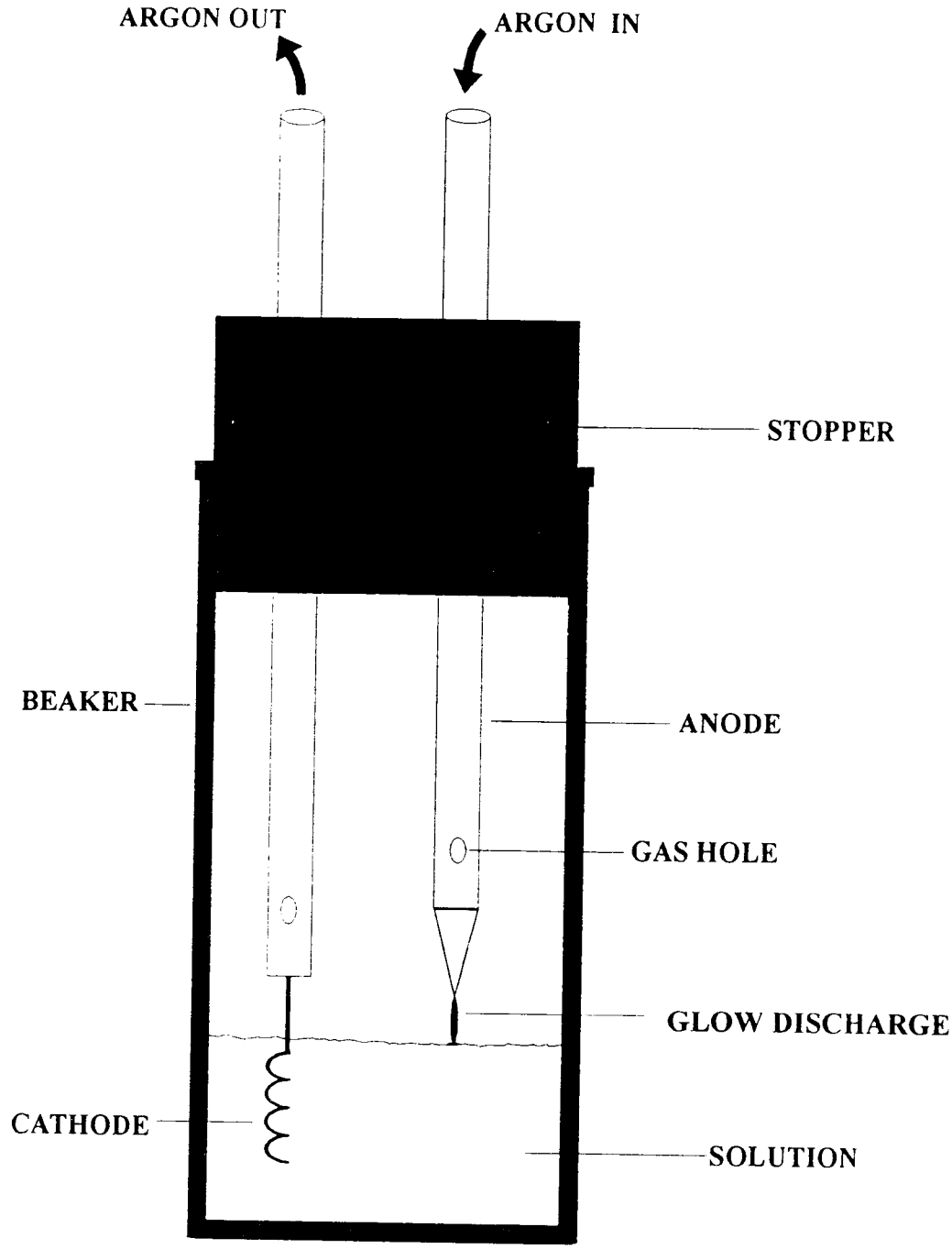

Figure 3.6. Diagram of the apparatus used for exposing solutions to a glow discharge with the solution acting as one of the discharge electrodes.

3.3.6 Nearby-Discharge Setup

The apparatus used for auxiliary experiments to expose solutions to the discharge operating between metallic electrodes is shown in figure 3.7. A 4-in length of 2-1/4-in.-o.d. x 2-in.-i.d. plexiglas tubing glued on one end to a 3-in diameter plexiglas disc is used as the glow discharge cell. Two pointed brass electrodes are supported by 1/4-in Ultra-Torr adapters, pressed through two holes drilled in the tube. Argon flows in the anode and out the cathode. The 25-ml beaker rests on a 1-1/2-in diameter plastic disc which rests in a water filled 3-1/2-in plastic petri dish. The Plexiglas tube also rests in this dish thus sealing the cell from the atmosphere. In each case the beaker is filled with 25.0 ml of solution and for all experiments the electrode spacing, discharge current, and solution-discharge distance are 1 cm, 2 mA, and 1 cm, respectively.

3.3.7 Hydrogen Peroxide Determination

Hydrogen peroxide is determined spectroscopically in irradiated solutions using the I_3^- method.[23] Two ml of a solution containing 0.4 M KI, 0.05 M NaOH, and 0.16 mM ammonium molybdate is mixed with 2 ml of 0.05 M potassium hydrogen phthalate directly in a standard 1-cm quartz cuvette. One ml of deionized water and 0.1 ml of irradiated sample solution are added and the solution is mixed. The absorbance is measured at 352 nm using a diode array spectrometer (Hewlett Packard, model 8452A). The blank

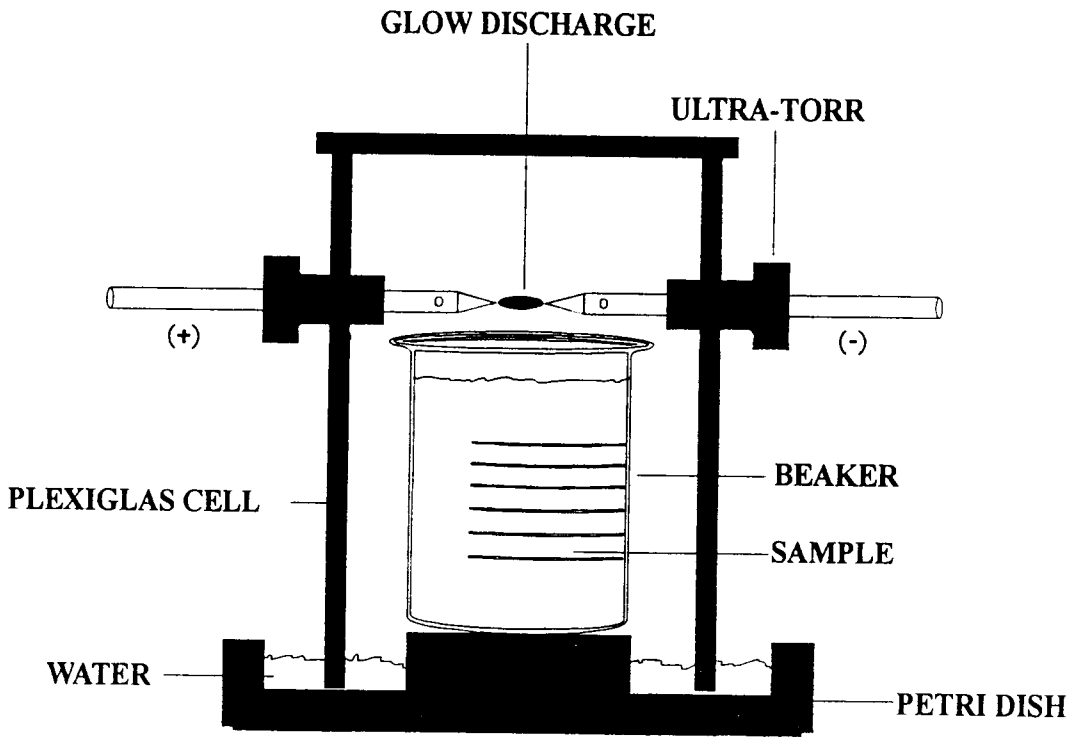

Figure 3.7. Diagram of the apparatus used for exposing solutions to a glow discharge operating between metallic electrodes.

consists of the above solutions with 0.1 ml doubly deionized water used instead of the sample. The technique is calibrated using a series of hydrogen peroxide standards made in doubly deionized water.

3.3.8 pH Determination

Acid concentration is determined by a pH meter (Orion, model 701A) equipped with a combination pH electrode (Orion, model 91-55). The meter is calibrated with pH 4.0 and 7.0 buffers (Metrepak, pHydroion). Each solution is allowed to equilibrate 2 min before a reading is taken. The exact identity of the acid or acids was not determined.

3.3.9 Absorbing Species

The diode array spectrometer is used to observe the absorbing species at 260 nm using a standard 1 cm quartz cuvette. Doubly deionized water is used as the blank.

3.3.10 Chemicals

Xylose, glucose, sucrose, lactose, melezitose, maltose, maltotetraose, and maltohexaose were obtained from Sigma and Aldrich. Fresh carbohydrate solutions were made before each analysis and all solutions were prepared in doubly deionized water. Hydrogen peroxide, potassium iodide, ammonium molybdate, potassium hydrogen phthalate, and sodium hydroxide were obtained from J.T. Baker and Sigma. All chemicals were of analytical reagent grade.

3.4 Results and Discussion

3.4.1 Liquid Cathode Products

Figure 3.8 shows plots of hydrogen peroxide, acid, and absorbing species formation vs glow discharge exposure time using the apparatus in figure 3.6 where the solution is the cathode. Three solutions of each glucose concentration were exposed to the glow discharge for 5, 10, and 15 min, respectively. Deionized water solutions were also exposed in a similar manner.

For all glucose concentrations the amounts of hydrogen peroxide, acid, and absorbing species increase with discharge exposure. The increase is linear for all hydrogen peroxide samples and for the most concentrated acid and absorbing species samples. The hydrogen peroxide and absorbing species plots all pass through the origin, and the acid plots intersect at approximately the same point (5 μM H_3O^+). The formation rates of hydrogen peroxide and acid, from lowest to highest glucose concentration, are 1.9, 1.4, 0.90, 0.47 and 0.005, 0.06, 0.20, 0.27 μmol min^{-1}, respectively. The absorbing species was not quantified and thus no formation rates where calculated. For a given discharge exposure, as the concentration of glucose increases the concentrations of acid and absorbing species increase, but the concentration of hydrogen peroxide decreases.

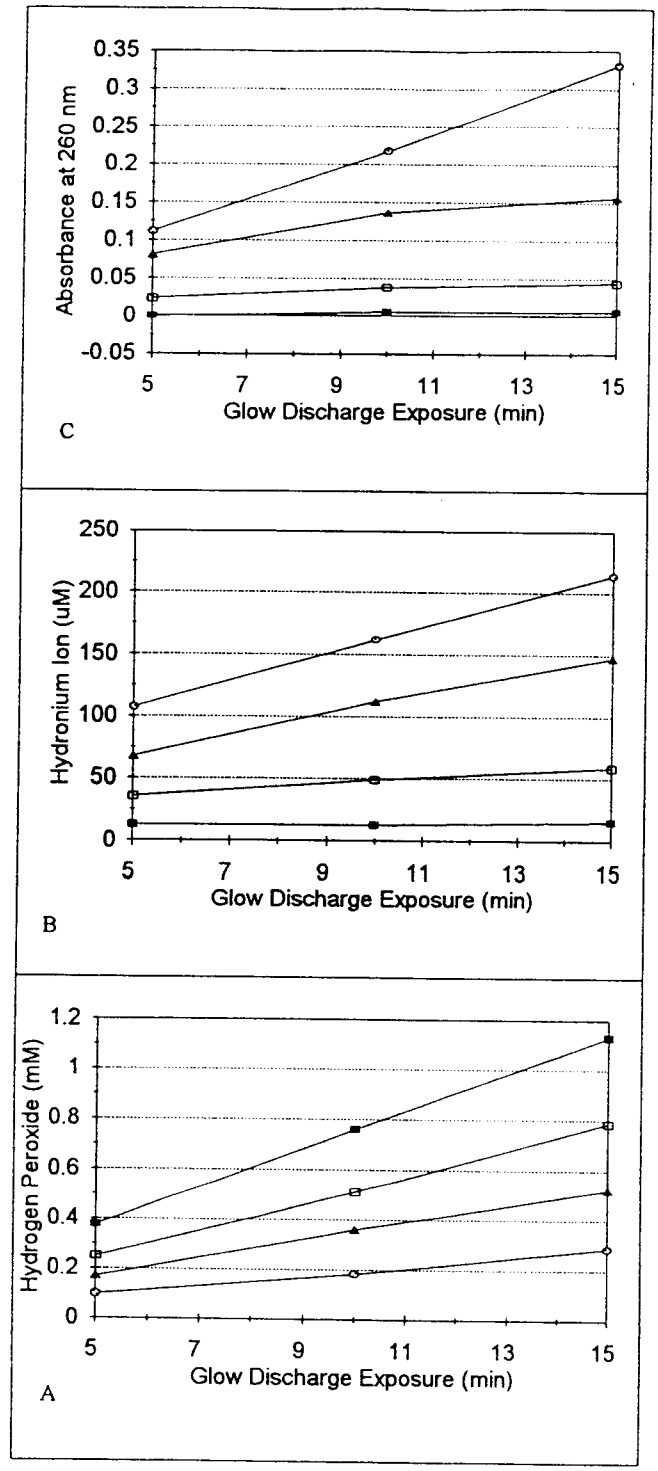

Figure 3.8. Formation of (A) hydrogen peroxide, (B) acid, and (C) absorbing species at various glow discharge exposure times and glucose concentrations. Water (■), 0.1 mM glucose (□), 1 mM glucose (▲), and 10 mM glucose (o).

There have been numerous studies in radiation chemistry which show strong similarities to the above behavior. Under similar conditions, yield vs radiation dose plots of hydrogen peroxide, acid, and malonic dialdehyde (absorbing species) are also linear.[18,20,25] The formation rates vary depending upon irradiation conditions but are generally within an order of magnitude indicated by the above data. Although absolute values for glow discharge doses were not determined for the above glow discharge experiments, dose is proportional to exposure time.

3.4.2 Liquid Cathode vs Liquid Anode Products

Figure 3.9 is a plot of hydrogen peroxide, acid, and absorbing species formation vs discharge exposure for six 0.01-M glucose solutions. Three of these solutions were exposed to the discharge for 5, 10, and 15 min using a liquid cathode and three were similarly exposed using a liquid anode. For each case the discharge current was 2 mA and all other conditions were constant.

It is evident that more hydrogen peroxide, acid, and absorbing species are formed if the solution is made a cathode than an anode. Similar trends in the concentrations of hydrogen peroxide and acid are seen if pure water solutions are exposed in the same manner. Concentrations of hydrogen peroxide, acid, and absorbing species all increase by factors of 2.3, 4.0, and 2.4, respectively, when switching from the liquid anode to liquid cathode. These

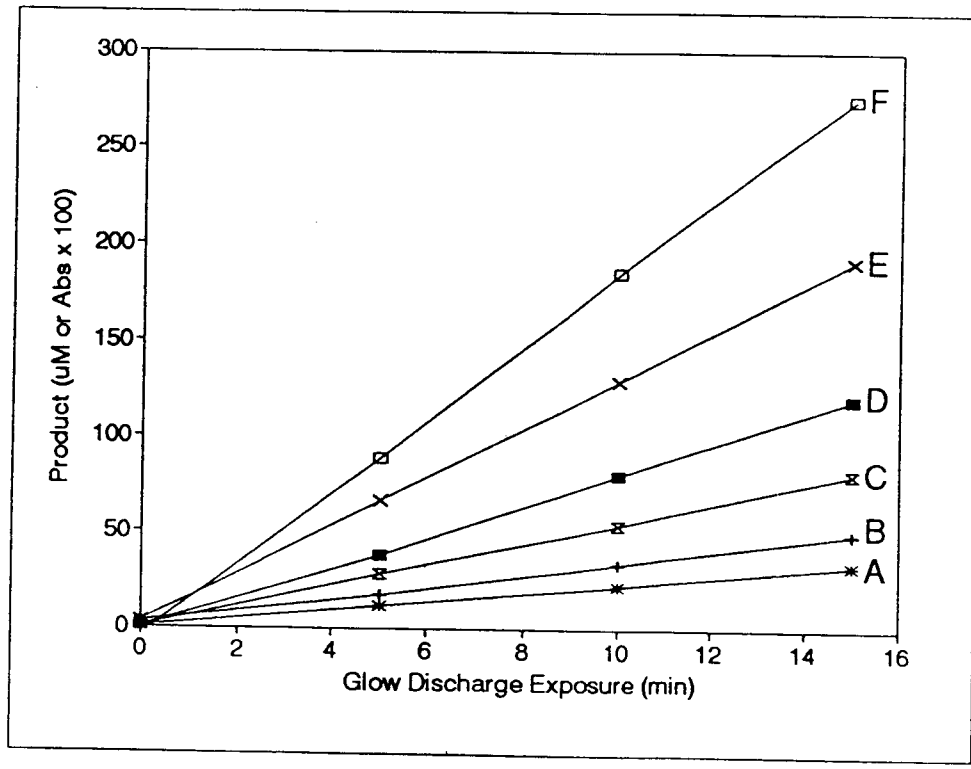

Figure 3.9. Normalized plot of hydrogen peroxide (D, liquid anode, F, liquid cathode), acid (B, liquid anode, E, liquid cathode), and absorbing species (A, liquid anode, C, liquid cathode) formation vs discharge exposure.

data suggest that the cathode is more efficient in bringing about product formation than the anode.

In a glow discharge the current at the cathode and anode is carried predominantly by positive ions and electrons, respectively. Most of the discharge voltage drop occurs near the cathode and only a fraction occurs near the anode. Typical values of the cathode and anode fall in an argon glow discharge are 200 V and 20 V, respectively.[26] It follows that the positive ions entering the solution (liquid cathode case) impart more energy to the solution than do electrons entering the solution (liquid anode case). Thus more product formation is expected when the solution is the cathode. Several authors[10-12] have used this model to explain the decreased oxidation yields of various aqueous metal ions when using a liquid anode vs a liquid cathode. The glow discharge electrolysis of aqueous glucose also seems to follow this model.

3.4.3 Discharge Products using Nearby-Plasma

Figure 3.10 shows a plot of hydrogen peroxide and acid formation vs discharge exposure using the apparatus shown in figure 3.7. A series of 0.01-M glucose solutions were exposed for 5, 10, 15, 30 and 76 min, respectively. Operating conditions are described in the experimental section.

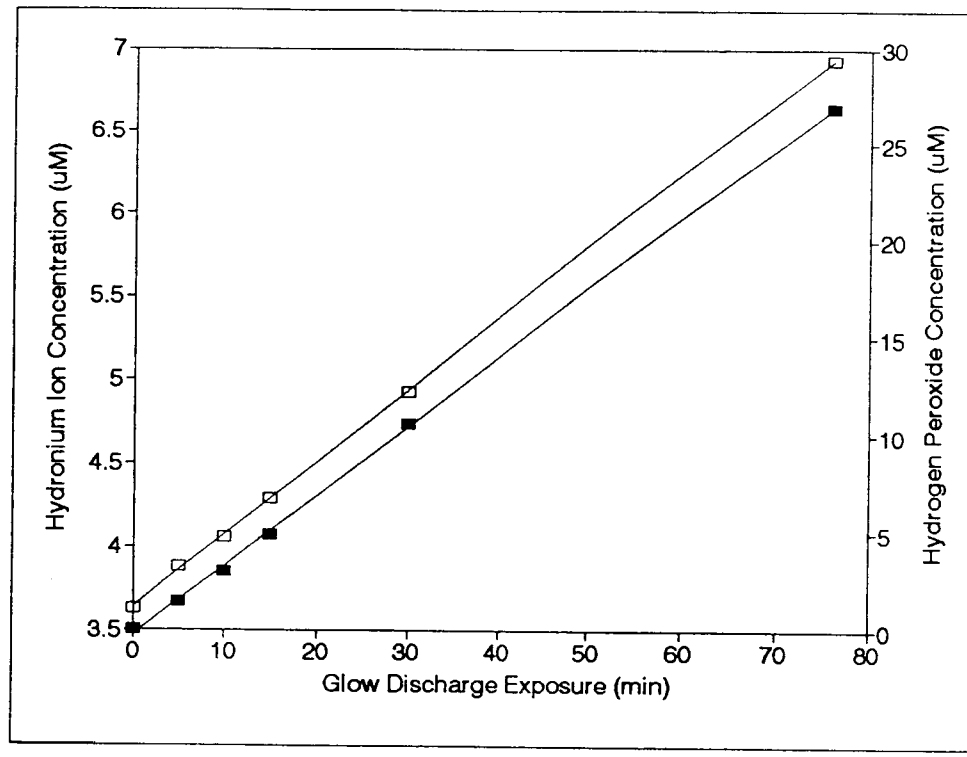

Figure 3.10. Hydrogen peroxide and acid formation for a 0.01-M glucose solution vs exposure using a nearby-glow discharge. Hydrogen peroxide (■), and acid (□).

The concentrations of hydrogen peroxide and acid increase linearly with discharge exposure with formation rates of 9 and 1 nmol min^{-1}, respectively. These are far less than the rates calculated using the liquid-interfaced discharge. There was also negligible production of the absorbing species and this was attributed to the large discharge-solution distance. More hydrogen peroxide, acid, and absorbing species formed as the discharge-solution distance was decreased and when the discharge was approximately 0.2 cm from the solution the rates of product formation approached those encountered with the liquid electrode. It was difficult to reduce the discharge-solution distance below 0.2 cm because the liquid extinguished the discharge. The formation of new products in any solution due to a glow discharge operating near a solution has not been observed until now.

3.4.4 Flowing Solution Products using Nearby-Plasma

Figure 3.11 shows plots of hydrogen peroxide, acid, and absorbing species formation vs flowing glucose solution concentration, using the apparatus in figure 3.1, for two flow rates. The flowing glucose concentration was increased by spiking the mobile phase reservoir with a known volume of 1.0 M glucose. As glucose passes the discharge it is continuously converted to an acid and collected in 20 ml glass vials. In all cases the discharge was operated with

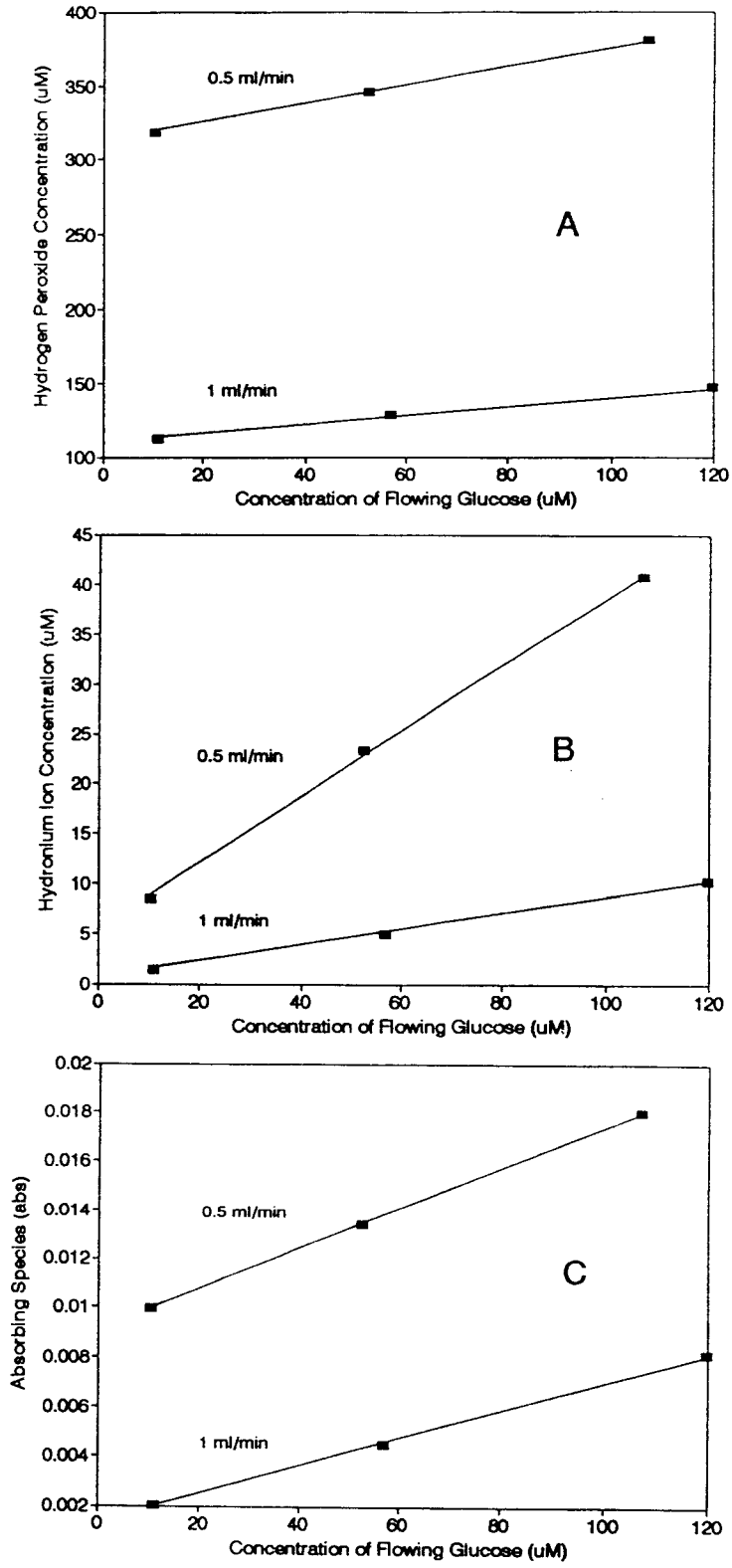

Figure 3.11. (A) hydrogen peroxide, (B) acid, and (C) absorbing species formation vs flowing glucose concentration using a glow discharge operating between metallic electrodes 2 mm from the flowing solution.

an electrode spacing, current, and discharge-solution distance of 2 mm, 2 mA, and 0.2 cm, respectively.

The concentration of hydrogen peroxide, acid, and absorbing species is linear with flowing glucose concentration. For 0.5 ml/min the hydrogen peroxide, acid, and absorbing species slopes are 0.65 mol H_2O_2/mol glucose, 0.33 mol H_3O^+/mol glucose, and 8 x 10^{-5} abs units/mol glucose, respectively. Similarly for 1 ml/min the slopes are 0.25 mol H_2O_2/mol glucose, 0.079 mol H_3O^+/mol glucose, and 6 x 10^{-5} abs units/mol glucose. A two fold decrease in flow rate results in a 4.2, 2.6, and 1.3 increase in acid, hydrogen peroxide, and absorbing species production, respectively. This is explained by the effective increase in glow discharge exposure at the lower flow rate. Longer exposure times yield larger amounts of products.

It is interesting to note that the increase in hydrogen peroxide with glucose concentration is opposite the results obtained with the liquid electrode experiments. The reason is not clear but the results are consistent with a well known reaction between OH radicals and glucose that yields hydrogen peroxide and acid.[18]

3.4.5 Nearby-Plasma Mechanism

The reason why hydrogen peroxide, acid, and absorbing species are formed when a glow discharge is operated near a stationary or flowing glucose solution is an important question. It is important to note that the solution as

shown in figure 3.7 does not conduct ordinary plasma current since there is no plasma electrode in contact with the solution. Thus the situation is fundamentally different than when the solution is made a conductive electrode where current is passed through the solution to a submerged metallic electrode. It is well known[26] that high-energy electrons and ions escape from glow discharges. It is also conceivable that high-energy photons emitted by the discharge could play a role in causing a response when a glow discharge is placed near a solution. However, experiments where a quartz encased atmospheric pressure argon glow discharge is run near to an aqueous solution yield no product formation, indicating that photons generated by the glow discharge are not responsible for product formation.

In order to study the nearby-glow discharge product formation mechanism the glow discharge-conductivity detector (figure 3.1) was interfaced to the HPLC (figure 3.3). The system was operated at 1 ml/min using pure doubly deionized water as the mobile phase. The glow discharge operated at 2 mA, had an electrode spacing of 1 mm, and was approximately 2 mm from the surface of the solution. 20-μL injections of a 500-μM glucose and 50-μM KCl solution where made at various outer brass cell potentials with respect to ground. The glucose was detected as an acid formed by exposure to the glow discharge. Under the above conditions, the KCl and glucose eluted at 1.7 and 3.2 min, respectively. The

purpose of adding KCl was to compensate for any physical changes at the conductivity detector interface that might change solution conductance. Taking the ratio of the glucose and KCl responses should compensate for this effect. The potential of the outer brass detector cell wall (figure 3.2) was varied with a power supply (Hewlett Packard, model 6516A, 0-3000 V).

Figure 3.12 shows chromatograms of KCl and glucose for cell wall potentials of +900, +400, and -400 V. As cell wall potential becomes more positive there is an increase in baseline conductivity, KCl response, and glucose response. All responses are measured as peak heights from baseline. The KCl response increases by the same percentage as the baseline for a given cell voltage increase. The reason why there is such an increase in KCl response is not known since KCl should not form any conductive products due to exposure to the glow discharge. The percentage increase in glucose response, however, is greater than the increase in KCl response as the wall potential is made more positive. Since a positive wall potential attracts plasma electrons and repels positive ions emitted from the plasma this indicates that positive ions from the plasma play a more important role than electrons in the formation of conductive solution products.

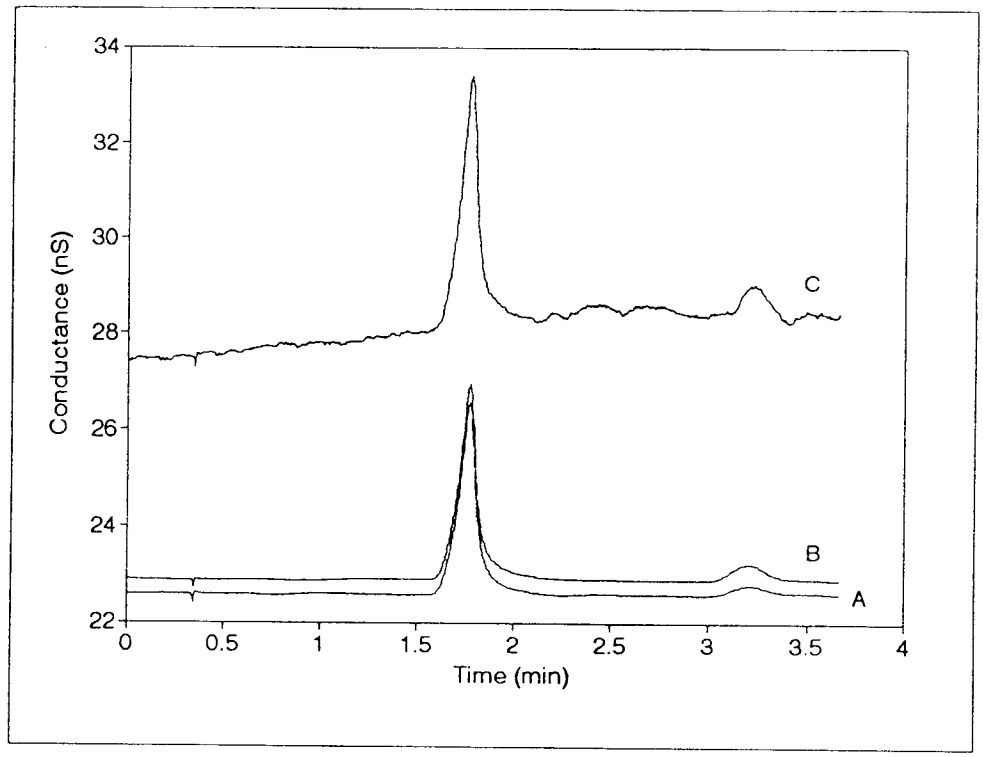

Figure 3.12. Chromatograms of KCl and glucose at brass cell potentials of (A) -400 V, (B) +400 V, and (C) +900 V.

3.4.6 OH Radical Scavenging Experiment

In radiation chemistry it is well known that OH radicals react readily with all carbohydrates[18] and are responsible for most of their decomposition. The dependence of the OH radical on product yield is typically studied by increasing or decreasing OH radical concentration through aqueous electron scavengers ($N_2O + H_2O^- \Rightarrow N_2 + \cdot OH + OH^-$) or OH radical scavengers ($I^- + \cdot OH \Rightarrow I\cdot + OH^-$)[18,27], respectively. For example, the concentration of malonic dialdehyde in X-ray or Gamma-ray irradiated glucose solutions is doubled if the solution is first saturated with nitrous oxide before radiolysis. Any product which is formed from OH radical reactions will be influenced in a similar manner. No study has investigated the interaction of OH radicals, formed in solution by a glow discharge, towards aqueous carbohydrates.

Figure 3.13 shows the chromatograms of two 20-μL, 100-μM glucose injections. The two injections were run in 50-μM potassium chloride (7.495 μS/cm) and 50-μM potassium iodide (7.515 μS/cm), respectively. Conditions between the two runs were constant and the discharge current was 1.5 mA.

Glucose response in 50-μM KI is approximately 50 % lower than the response in 50-μM KCl. This is within 10 % of the ratio of rate constants for the competing scavenging reactions ($\cdot OH + Cl^-$, $\cdot OH + I^-$).[18] Thus it appears that OH radical is generated in solution by the nearby-glow discharge and is important in the formation of acidic product.

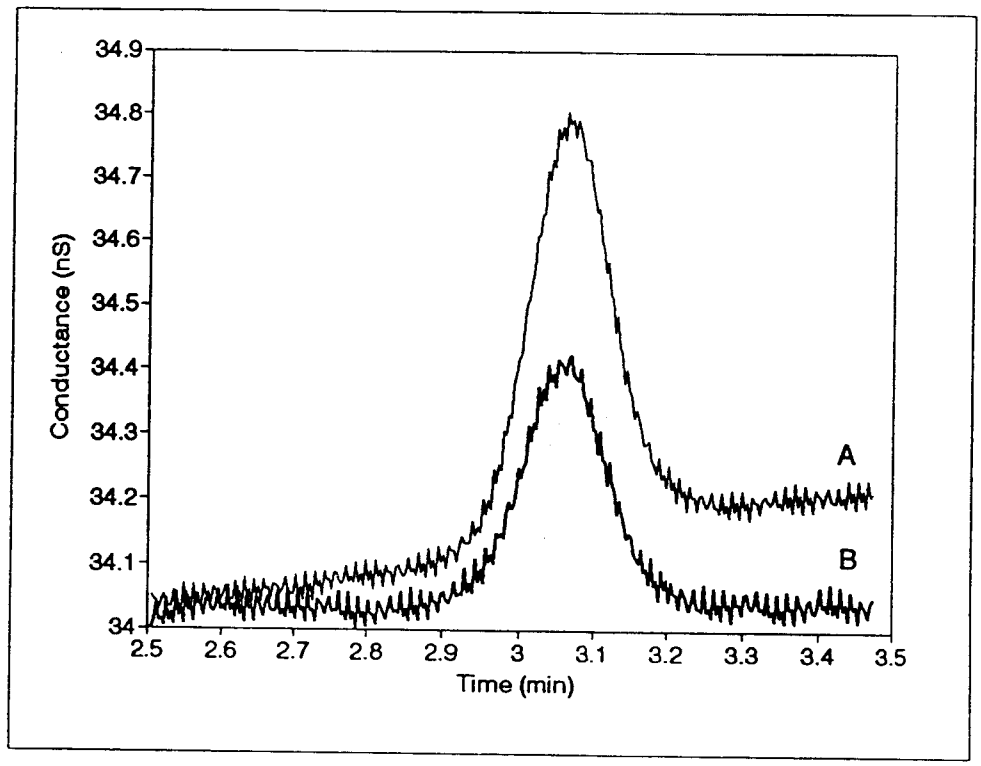

Figure 3.13. 100-μM glucose injections in (A) 50-μM KCl and (B) 50-μM KI.

3.4.7 Discharge Electrode Spacing vs Response

Figure 3.14 shows a plot of peak height, signal-to-noise ratio, and baseline conductance vs discharge electrode spacing for a series of 20-μL, 100-μM glucose injections. The glow discharge current was kept at 2 mA and the liquid flow rate at 1 ml/min for all electrode spacings. Average baseline conductance and noise where determined by calculating the average and standard deviation in 50 points of each baseline, respectively.

As electrode spacing increases peak height, baseline conductance, and S/N increase until approximately 2 mm where they level off. The leveling effect occurs when the electrode spacing approximately equals the width of the liquid flowing down the glass slide. No change in the area of the flowing liquid was noted with increasing electrode spacing suggesting that glow discharge area is an important parameter in determining sensitivity. The fact that baseline conductance follows the response indicates that the same phenomena causing the glucose oxidation is causing the changes in background conductance. A larger discharge area exposes the flowing solution to more ions and electrons per unit time thus increasing solution decomposition. Electrode spacings above approximately 4 mm result in excessive noise and arcing to the outer brass cell.

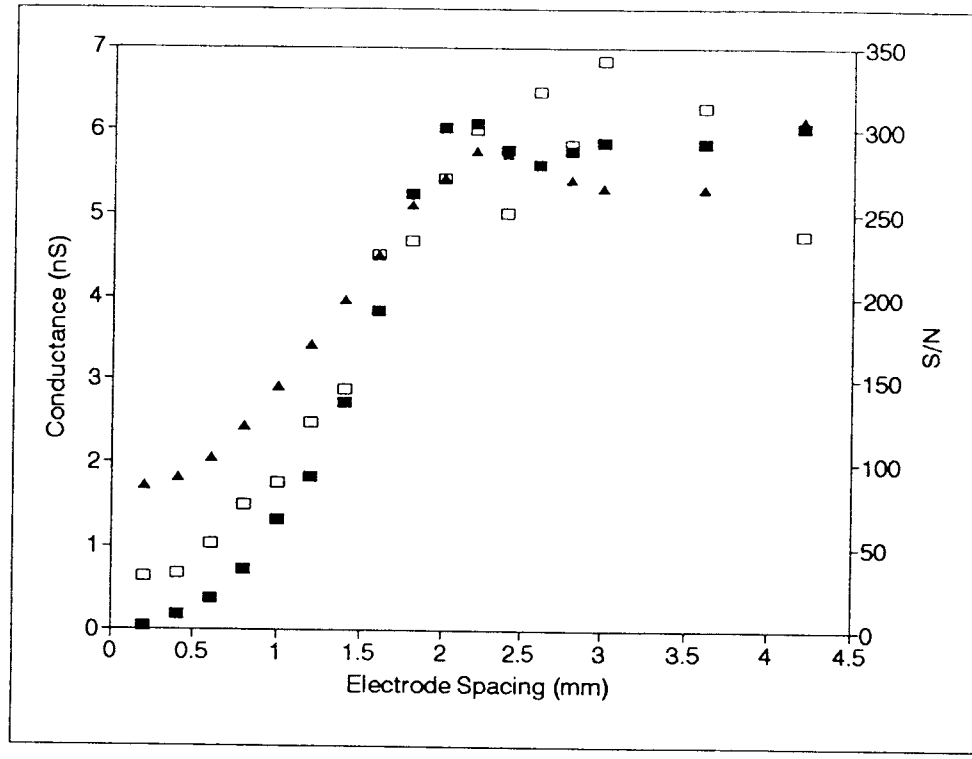

Figure 3.14. Baseline (▲), peak height (■), and S/N (□) vs electrode spacing for 100-μM glucose injections.

3.4.8 Effect of Discharge Current on Response

Figure 3.15 shows a plot of peak height and detector noise vs glow discharge current for a series of 20-μL, 100-μM glucose injections. For all runs the electrode spacing was 1 mm and all other conditions were the same as above.

As discharge current increases there is an increase in response and noise and no significant improvement in the signal-to-noise ratio. One possibility is that increasing discharge currents produce increasing heat and detector noise. At approximately 10 mA an indentation, approximating the shape of the pointed cathode, was formed in the flowing solution near the cathode, and an increase in current further enlarged this indentation. The reason this occurred was not clear but could have to do with the strong electric field lines emanating from the pointed cathode. Since most of the plasma energy is dissipated near the cathode, solution heating is a potential cause. The overall effect was to reduce the area of the flowing solution near the discharge and would explain the signals leveling at 10 mA. The optimum value for discharge current was 2 mA and any lower or higher than this value caused discharge instabilities and excessive solution heating, respectively.

3.4.9 Effect of Discharge-Solution Distance

Figure 3.16 shows chromatograms of four 20-μL, 100-μM glucose injections, each run at a different glow discharge-solution distance. For each case the flow rate, discharge

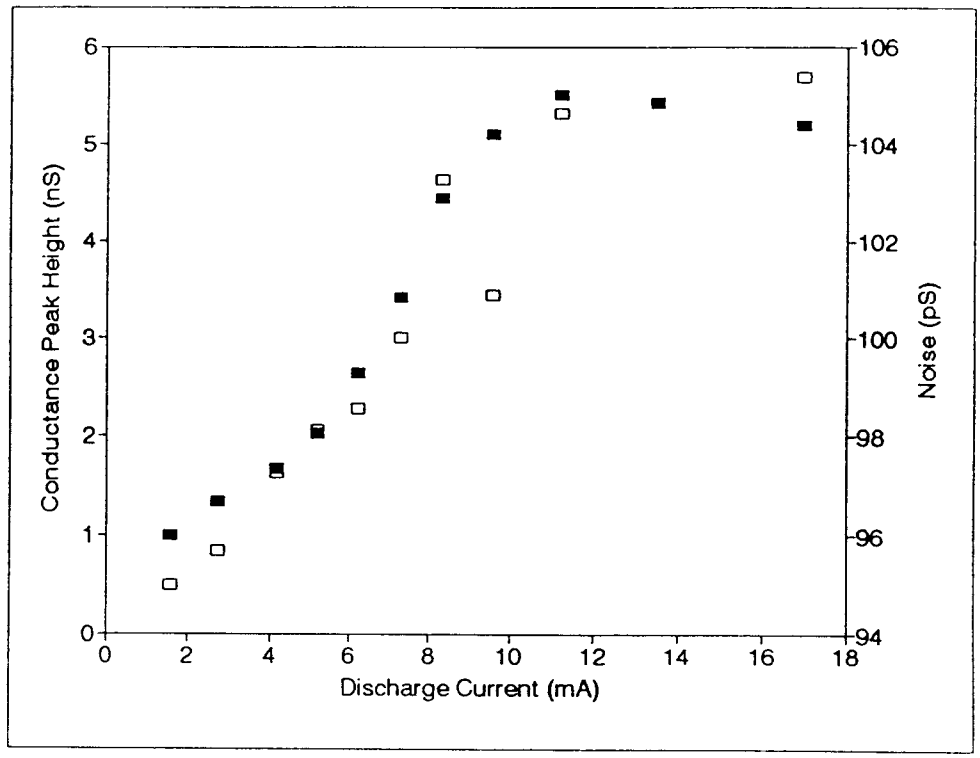

Figure 3.15. Peak height (■), and noise (□) vs discharge current for 100-μM glucose injections.

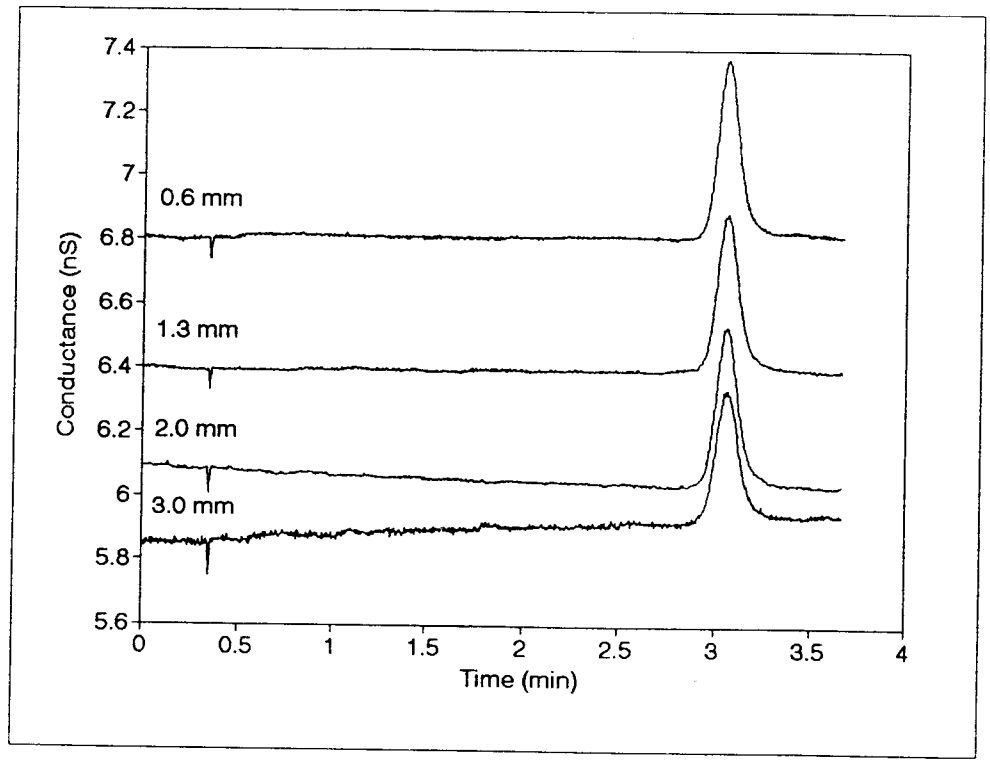

Figure 3.16. 100-μM glucose response for four discharge-solution distances.

current, and electrode spacing was 1 ml/min, 2.0 mA, and 1 mm, respectively.

As discharge-solution distance increased from 0.6 to 3.0 mm the signal-to-noise ratio remained approximately constant until 3.0 mm where it dropped by a factor of two because of increased baseline noise. Decreasing the discharge-solution distance below 0.2 cm resulted in discharge extinguishment. The discharge-solution distances yielding the optimal signal-to-noise ratios ranged from 0.6 to 2.0 mm.

3.4.10 Effect of Liquid Flow Rate on Response

Figure 3.17 shows 20-μL injections of 10-μM KCl (top) and 100-μM glucose (bottom), respectively. Each chromatogram was obtained at flow rates of 0.5 and 1 ml/min. For this study the C-18 column was placed before the injector to minimize dispersion, and the injector was connected directly to the detector. For all injections the glow discharge current, electrode spacing, and discharge-solution distance were 2 mA, 1 mm, and 2 mm, respectively. Potassium chloride was chosen because it is an inert electrolyte and should not be affected by the presence of the discharge.

For an ideal concentration detector, a two-fold decrease in flow rate will yield a two-fold increase in peak area and no change in peak height.[28] The potassium chloride injections approximate this behavior with the only

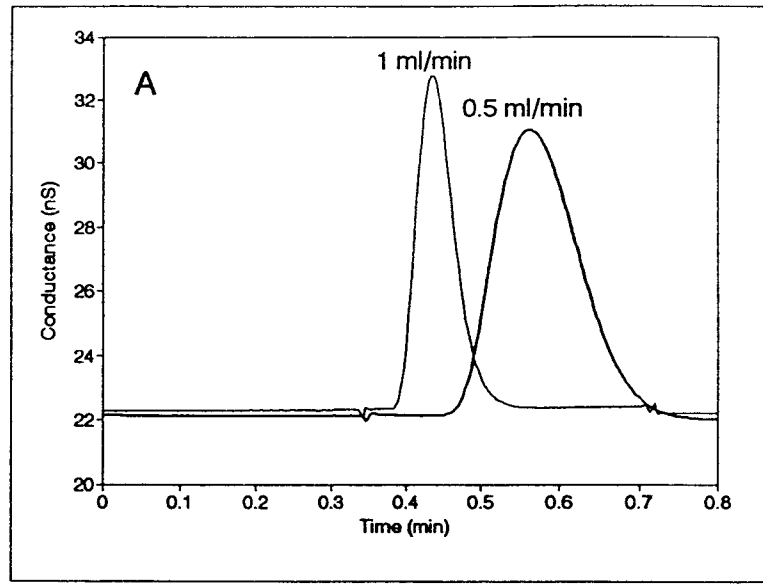

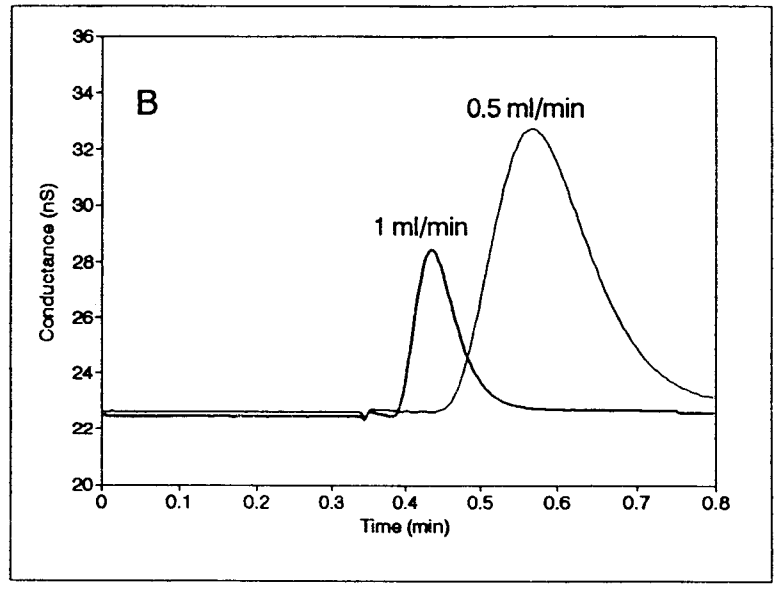

Figure 3.17. (A) 10-μM KCl injections and (B) 100-μM glucose injections, each at 0.5 and 1 ml/min flow rates.

discrepancy being a slight decrease in peak height at the lower flow rate. The glucose injections, however, do not follow the behavior predicted for a concentration detector. A two-fold decrease in flow rate increases the peak area and peak height by factors of 4.0 and 2.0, respectively. These data are reasonable since at a slower flow rate more ions and electrons hit the solution per unit time thus increasing the amount of product formed. Thus the detector behaves as a new type of detector and does not exhibit the properties of either a concentration or mass detector. This detector could be called a residence-time detector because the response increases with residence time in the detector.

3.4.11 Detector Calibration

Figure 3.18 shows two calibration curves, each at a different flow rate, created from 20-μL injections of 0.1, 0.5, 0.8, 1, 5, 10, 50, and 100-μM glucose. In both cases linearity extends over three orders of magnitude with negative deviation occurring above 100-μM. Taking two times the standard deviation of 50 baseline points and dividing by the calibration slope yields concentration detection limits of 30 and 70 nM for flow rates of 0.5 and 1 ml/min, respectively. Assuming a detector volume of 10-μL yields an in-cell mass detection limit of 40 and 100 fmol for 0.5 and 1 ml/min, respectively. Baseline noise was approximately the same for both flow rates. Both detection limits are

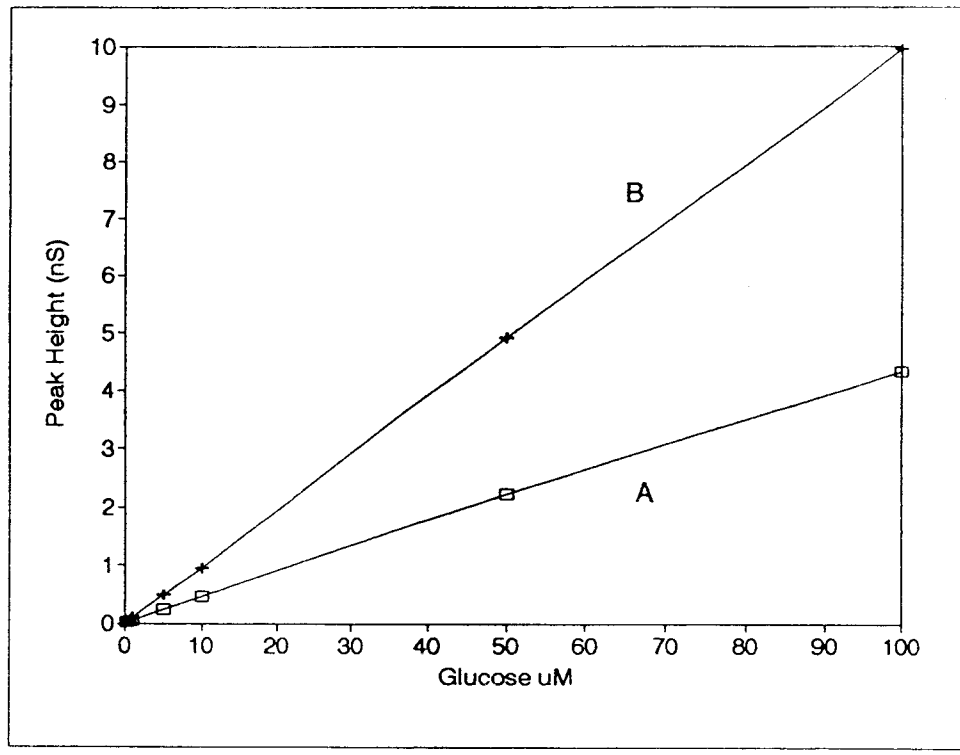

Figure 3.18. Glucose calibration at flow rates of (A) 1 ml/min and (B) 0.5 ml/min.

comparable to the most sensitive methods currently available for carbohydrate detection.[6,7]

Figure 3.19 shows calibration curves for xylose, glucose, sucrose, lactose, and melezitose each obtained with a flow rate of 1 ml/min. Concentration detection limits are 90, 70, 50, 50, and 60 nM for xylose, glucose, sucrose, lactose, and melezitose, respectively. The linearity in each case extends over three orders of magnitude with negative deviation occurring above 100-μM. The lower calibration slopes for xylose and glucose indicate that response could depend on the type of carbohydrate. It has been shown in radiation chemistry that disaccharides and polysaccharides have slightly higher acid yields than monosaccharides.[18]

3.4.12 Effect of Electrode Spacing on Linearity

Figure 3.20 shows log-log glucose calibration plots at different discharge electrode spacings. The current was maintained at 2 mA for all electrode spacings and the flow rate was 1 ml/min. The response indices[34] for electrode spacings of 0.1, 0.3, 0.5, and 1 cm are 0.40, 0.81, 0.86, and 0.98, respectively, indicating that larger electrode spacings result in a more linear response. As discharge area increases the detector system is able to more efficiently handle the rates of conversion necessary for a linear response. Thus for a reasonable linear range (three orders of magnitude), the electrode spacing must be above 1

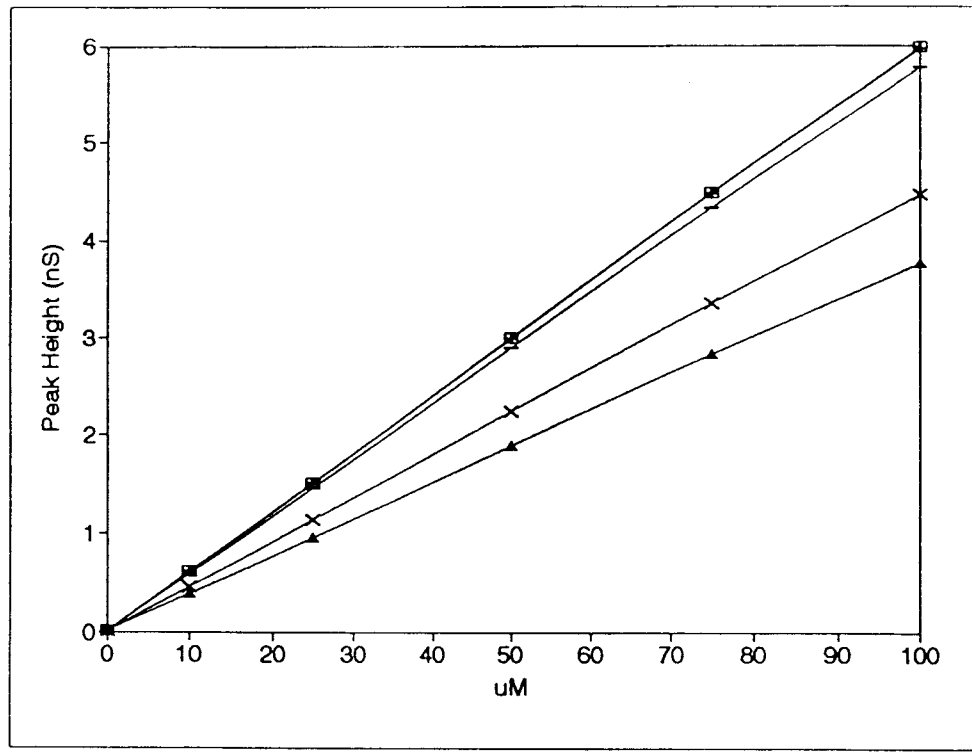

Figure 3.19. Carbohydrate calibration curves. Melezitose (-), sucrose (□), xylose (▲), lactose (+), and glucose (x).

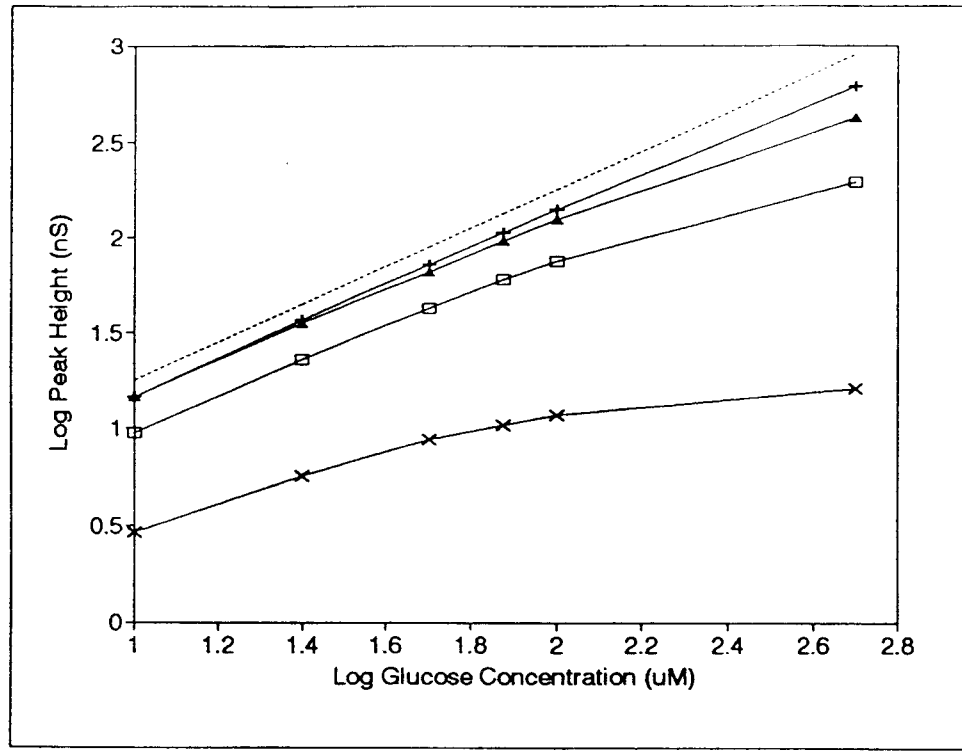

Figure 3.20. Effect of calibration linearity on glow discharge electrode spacing. Spacings: 0.1 (X), 0.3 (□), 0.5 (▲), and 1 cm (+). Slope of unity (---) is shown for comparison.

cm. These data indicate that it is possible to extend the linear range by using larger electrode spacings or multiple discharges in parallel. One problem which develops at very large electrode spacings (> 1.5 cm) is discharge wandering on the electrodes, which causes excessive noise. No such problems are encountered with dual glow discharges operating in parallel near the flowing solution. In such cases we have found that doubling the discharge area, by introducing another identical discharge in parallel, doubles the sensitivity and linearity.

3.4.13 Mobile Phase Compatibility

Figure 3.21 shows chromatograms for a series of 6-μL, 200-μM glucose injections obtained with water, methanol, ethanol, acetone, and acetonitrile mobile phases. These solvents where chosen to represent common solvents used in liquid chromatography. Most organic solvents are OH radical scavengers and decrease the concentration of OH radicals. The OH radical rate constants for acetonitrile, acetone, methanol, and ethanol are 2.2×10^4, 11×10^4, 97×10^4, and 190×10^4 $m^3\ mol^{-1}s^{-1}$, respectively.[29]

Glucose response decreases with increasing organic solvent OH radical rate constant. There is a 40% decrease in peak height when changing from a pure water mobile phase to 0.1 % acetonitrile. At the typical acetonitrile concentrations (60-80%) used in the separation of carbohydrates by liquid chromatography, there is a complete

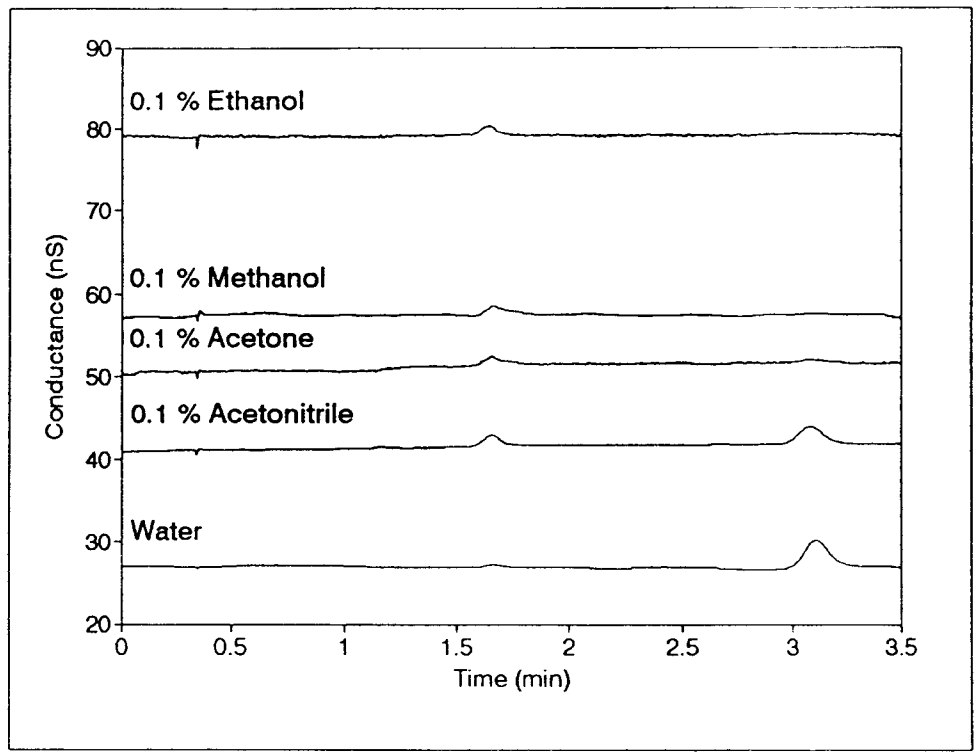

Figure 3.21. Effect of mobile phase composition on 200-μM glucose response. The first peak, at 1.6 minutes, is caused by conductive impurities in the injection sample, most likely dissolved carbon dioxide. The second peak, at 3.1 minutes, is glucose.

loss of signal, even for very concentrated glucose injections. In addition, the use of 1-100 % acetonitrile solutions causes the rapid formation of a black material on the electrodes which eventually extinguishes the discharge. Aqueous solutions of methanol, ethanol, and acetone also quench the signal but do not affect the stability of the glow discharge significantly. Thus the use of organic solvents is detrimental to the analysis of carbohydrates using the glow discharge-conductivity detector. The detector works best with a pure water mobile phase which is typical for carbohydrate analysis by ligand exchange chromatography.[4,6,30]

3.4.14 Carbohydrate Separation

Figure 3.22 shows a chromatogram from a 6-μL injection of 100-μM glucose, 80-μM maltotetraose, and 50-μM maltohexaose obtained on the C-18 column with a flow rate of 0.5 ml/min pure water. The separation conditions are typical for the analysis of oligosaccharides using a C-18 type column.[6,31-33]

3.5 Conclusions

It has been shown that when a glow discharge is operated between metallic electrodes near an aqueous glucose solution, or interfaced directly to the solution, hydrogen peroxide, acid, and absorbing species are formed in amounts proportional to glow discharge exposure. The products

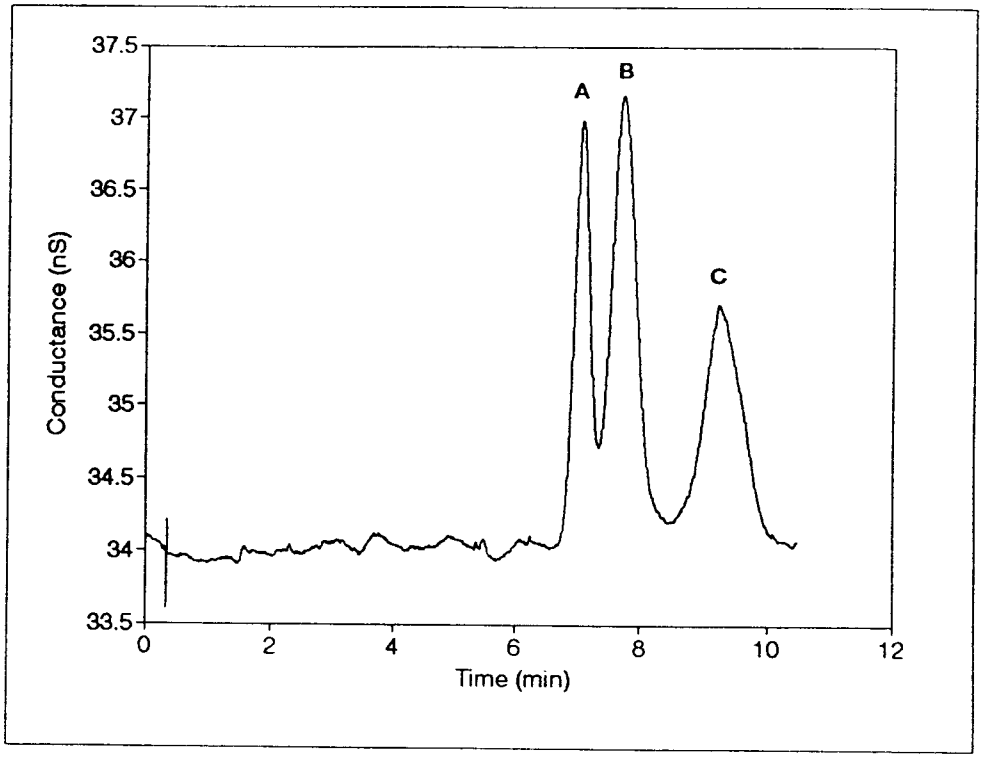

Figure 3.22. Chromatograms of (A) 100-μM glucose, (B) 80-μM maltotetraose, and (C) 50-μM maltohexaose.

formed are similar to those formed during the high energy radiolysis of aqueous carbohydrates.

The new HPLC-interfaced-glow discharge-conductivity detector is capable of detecting carbohydrates, via their acidic decomposition products, at low nanomolar and femtomole levels. The sensitivity competes with the most sensitive techniques available for the analysis of carbohydrates. The sensitivity and linearity may be improved further by using multiple glow discharges. In addition the carbohydrate detector is compatible with ligand exchange chromatography which uses pure water as the mobile phase.

Future studies will focus on the improvement of carbohydrate detection limits and the analysis of real glycoprotein samples. The possibilities of monitoring the UV absorbing products alone or in conjunction with conductivity will also be investigated. Monitoring both could lead to structural information since yields are to some extent determined by the structure of the carbohydrate.

Studies of other important compounds are also planned. For example, it has been found that part-per-billion levels of chloroform can be detected with the HPLC-interfaced-glow discharge-conductivity detector using pure water or methanol as the mobile phase.

3.6 References

[1] Sharon, N.; Lis, H. *Sci. Amer.* 1993, January, 82-89.

[2] Paulson, J.C. *TIBS*, 1989, 14, 272-276.

[3] Hardy, M.R., Townsend, R.R.; Lee, Y.C. *Anal. Biochem.* 1988, 170, 54-62.

[4] Stefansson, M; Westerlund, D. *J. Chromatogr. A* 1996, 720, 127-136.

[5] Paulus, A.; Klockow, A. *J. Chromatogr. A* 1996, 720, 353-376.

[6] Rassi, Z.E. *Carbohydrate Analysis. High Performance Liquid Chromatography and Capillary Electrophoresis*, Journal of Chromatography Library, Vol. 58, Elsevier: New York, 1995.

[7] Churms, S.C.; Sherma, J. *Carbohydrates: CRC Handbook of Chromatography Volume II*, CRC Press: Boston, 1991.

[8] Parriott, C.; Parriott, D. *A Practical Guide to HPLC Detection*, Academic Press: San Diego, 1993; Chapter 9.

[9] Herring, C.J.; Piepmeier, E.H. *Anal. Chem.* 1995, 67, 878-884.

[10] Hickling, A.; Denaro, A.R. *J. Electochem. Soc.* 1958, May, 265-270.

[11] Hickling, A.; Bockris, J.O'M.; Conway, B.E. *Modern Aspects of Electrochemistry*, Plenum Press: New York, 1971, 329-404.

[12] Hickling, A.; Ingram, M.D. *J. Electroanal. Chem.* 1964, 8, 65-81.

[13] Bullock, A.T.; Gavin, D.L.; Ingram, M.D. *J.C.S. Faraday I*, 1980, 76, 648-653.

[14] Sargent, F.P.; Gardy, E.M. *Canad. J. Chem.* 1976, 54, 275.

[15] Harada, K.; Suzuki, S.; Ishida, H. *Biosystems*, 1978, 10, 247-251.

[16] Harada, K.; Suzuki, S. *Nature*, 1977, 266, 275-276.

[17] Harada, K.; Iwasaki, T. *Nature*, 1974, 250, 427-428.

[18] Kocketkov, N.K.; Kudrjashov, L.I.; Chlenov, M.A. *Radiation Chemistry of Carbohydrates*, Pergamon Press: New York, 1979.

[19] Bothner-By, C.T.; Balazs, E.A. *Rad. Res.* 1957, 6, 302-317.

[20] Phillips, G.O. *Rad. Res.* 1963, 18, 446-460.

[21] Wolfrom, M.L.; Binkley, W.W.; McCabe, L.J.; ShenHan, T.M.; Michelakis, A.M. *Rad. Res.* 1959, 10, 37-47.

[22] Phillips, G.O. *Nature*, 1954, May, 1044-1045.

[23] Klassen, N.V.; Marchington, D.; McGowan, C.E. *Anal. Chem.* 1994, 66, 2921-2925.

[24] Ahmon, M. *Electronics*, 1977, Sept. 15, 132-133.

[25] Phillips, G.O.; Moody, G.J.; Mattok, G.L. *Rad. Res.* 1958, 3522-3534.

[26] Brown, S.C. *Basic Data of Plasma Physics*, John Wiley & Sons: New York, 1959.

[27] Phillips, G.O.; Griffiths, W.; Davies, J.V. *J. Chem. Soc.* (B), 1966, 194-200.

[28] Miller, J.M. *Chromatography: Concepts and Contrasts*, John Wiley & Sons: New York, 1988.

[29] Spinks, J.W.T.; Woods, R.J. *An Introduction to Radiation Chemistry*, 3rd ed.; John Wiley & Sons: New York, 1990.

[30] Davankov, V.A.; Navratil, J.D.; Walton, H. F. *Ligand Exchange Chromatography*, CRC Press: Florida, 1988.

[31] Cheetham, N.W.; Teng, G. *J. Chrom.*, 1984, 336, 161-172.

[32] Cheetham, N.W.; Sirimanne, P.; Day, W.R. *J. Chrom.*, 1981, 207, 439-444.

[33] Cheetham, N.W.; Sirimanne, P. *J. Chrom.*, 1981, 208, 100-103.

[34] Scott, R.P.W., *Liquid Chromatography Detectors*, 2nd ed.; Elsevier: New York, 1986.

Chapter 4

CONCLUSIONS

This thesis has shown the development of two aqueous carbohydrate detectors for flowing liquid systems implementing an atmospheric pressure argon glow discharge. In both cases the glow discharge is stable, easy to maintain, consumes little power, and is easily constructed.

Both glow discharge oscillation frequency and discharge current were used to detect micromolar and picomole quantities of sucrose in a flow injection system using the liquid-interfaced detector. The visual appearance of the glow discharge at various electrode spacings was discussed along with the nature of the oscillations and the possible reasons for response.

Shortly after the article on the liquid-interfaced detector was published, it was confirmed that the sucrose response was due to the formation of an acid, formed by sucrose decomposition from exposure to the glow discharge. It was concluded that the best way to monitor the acid in an aqueous flowing system was to use a conductivity detector, located down stream from the glow discharge. Further studies revealed that an acid was formed whether the discharge was interfaced directly to the solution, or operated between metallic electrodes near the solution. The advantage of operating the discharge near to the solution was a dramatic reduction in conductivity detector noise.

This new type of detector, where the discharge operates near the flowing solution with a conductivity detector located downstream from the discharge, is called the glow discharge-conductivity detector. This detector has been shown to detect nanomolar and femtomole quantities of a variety of carbohydrates including glucose, sucrose, xylose, melezitose, lactose, maltotetraose, and maltohexaose. The parameters which govern detector sensitivity such as discharge electrode spacing, discharge current, and liquid flow rate have been discussed. In general, increasing the discharge electrode spacing or decreasing the liquid flow rate leads to an increase in sensitivity, since discharge area and solution exposure time are being increased, respectively. In addition, multiple parallel glow discharges have been shown to yield higher sensitivities due to the increased discharge area. It was also shown that the linearity of response depends on the electrode spacing, and larger electrode spacings lead to a more linear response. The detector is also compatible with carbohydrate analysis by ligand exchange chromatography, which is growing in popularity because it uses pure water as the mobile phase, and not the highly toxic acetonitrile, most commonly used in carbohydrate analysis.

The products formed from exposure of aqueous carbohydrates to a glow discharge are similar to those formed when exposed to high energy radiation such as X-rays or gamma-rays. In general, when an aqueous carbohydrate is

exposed to a glow discharge it is oxidized by aqueous hydroxyl radicals, formed in solution from the impinging electrons and argon ions. The carbohydrate yields an acid and absorbing species in amounts proportional to carbohydrate concentration and discharge exposure time.

The glow discharge-conductivity detector competes with the sensitivity and linearity of the pulsed amperometric detector, which is considered to be the most sensitive commercially available carbohydrate detector available. This detector exhibits nanomolar detection limits and has a linear range of 10^3. The increased interest in carbohydrate moieties attached to glycoproteins has pushed the sensitivity requirements of the pulsed amperometric detector even lower. Thus the glow discharge-conductivity detector could prove useful to the analysis of very low levels of carbohydrates as encountered in glycoprotein analysis.

Future work on the glow discharge-conductivity detector will include improvement of its sensitivity and linearity by using multiple parallel glow discharges. Determination of the detector conversion efficiency (moles carbohydrate consumed / moles acid formed) for various carbohydrates is important since this eventually limits detector sensitivity. The monitoring of UV products, with a UV detector, either alone or in conjunction with conductivity should be investigated to examine any sensitivity enhancement or any structurally significant information about the carbohydrate. The analyses of real glycoprotein samples and the response

to other important compounds are also planned. For example, chloroform has been detected at part-per-billion levels in a 70/30 methanol-water mobile phase using reverse phase HPLC and glow discharge-conductivity detection. In radiation chemistry it is well known that chloroform breaks down into hydrochloric acid when exposed to high energy radiation. The primary reactive species responsible is the hydrated electron which reacts readily with all chlorinated organics but not with common organic solvents such as methanol. Thus chlorinated organics could be analyzed using the glow discharge-conductivity detector with a purely aqueous or largely organic mobile phase. It would be interesting to try more toxic chlorinated hydrocarbons such as pesticides.

BIBLIOGRAPHY

Ahmon, M. *Electronics*, 1977, Sept. 15, 132-133.

Allen, A.O. *The Radiation Chemistry of Water and Aqueous Solutions*; Van Nostrand: New York, 1961.

Barshick, C.M.; Duckworth, D.C.; Smith, D.H. *J. Am. Soc. Mass Spect.* 1993, 4, 38.

Bellar, T.A.; Budde, W.L.; Kryak, D.D. *J. Am. Soc. Mass Spect.* 1994, 5, 908.

Bockris, J.O.; Conway, B.E.; Hickling, A. *Modern Aspects of Electrochemistry*, No.6, Plenum Press: New York, 1971, 329-404.

Bothner-By, C.T.; Balazs, E.A. *Rad. Res.* 1957, 6, 302-317.

Broekaert, J.A.C., *J. Anal. At. Spectrom.* 1987, 2, 537.

Brown, S.C. *Basic Data of Plasma Physics*, John Wiley & Sons: New York, 1959.

Bullock, A.T.; Gavin, D.L.; Ingram, M.D. *J.C.S. Faraday I*, 1980, 76, 648-653.

Carazzato D.; Bertrand, M.J. *J. Am. Soc. Mass Spect.*, 1994, 5, 299.

Cheetham, N.W.; Teng, G. *J. Chrom.*, 1984, 336, 161-172.

Cheetham, N.W.; Sirimanne, P.; Day, W.R. *J. Chrom.*, 1981, 207, 439-444.

Cheetham, N.W.; Sirimanne, P. *J. Chrom.*, 1981, 208, 100-103.

Churms, S.C.; Sherma, J. *Carbohydrates: CRC Handbook of Chromatography Volume II*, CRC Press: Boston, 1991.

Crookes, W., *Phil. Trans.*, Pt. I, 1879b, p. 152.

Cserfalvi, T.; Mezei, P.; Apai, P. *J. Appl. Phys. D.*, 1993, 26, 2184.

Cserfalvi, T.; Mezei, P.J. *Anal. At. Spectrom.* 1994, 9, 345-349.

Davankov, V.A.; Navratil, J.D.; Walton, H. F. *Ligand Exchange Chromatography*, CRC Press: Florida, 1988.

Davy H. Phil. Trans., 1821, 111, 427.

Denaro, A.R.; Owens, P.A., *Electrochim. Acta*, 1968, 13, 157.

Denaro, A.R.; Hickling, A., *J. Electrochem. Soc.*, 1958, May, 265.

Dewhurst, H.A.; Flagg, J.F.; Watson, P.K., *J. Electrochem. Soc.*, 1959, April, 366.

Donahue, T.; Dieke, G.H. *Phys. Rev.* 1951, 81, 248-261.

Eliezer, Yaffa; Eliezer, S. *The Fourth State of Matter: An Introduction to the Physics of Plasma*, Adam Hilger: Philadelphia, 1989.

Faraday, M., *Res. Elec.*, 1839, 663.

Gilbert, W., De Magnete, *Magneticisque Corporibus*, Petrus Short, London, 1600.

Goldstein, E., *Berl. Monat.*, 1876, 283.

Harada, K.; Suzuki, S.; Ishida, H. *Biosystems*, 1978, 10, 247-251.

Harada, K.; Suzuki, S. *Nature*, 1977, 266, 275-276.

Harada, K.; Iwasaki, T. *Nature*, 1974, 250, 427-428.

Hardy, M.R., Townsend, R.R.; Lee, Y.C. *Anal. Biochem.* 1988, 170, 54-62.

Harley, J.; Pretorius, V. *Nature*, 1956, 178, 1244.

Harrison, W.W.; Hess, K.R.; Marcus, R.K. *Anal. Chem.*, 1986, 58, 341A.

Herring, C.J.; Piepmeier, E.H. *Anal. Chem.* 1995, 67, 878-884.

Hickling, A.; Ingram, M.D. *J. Electroanal. Chem.* 1964, 8, 65-81.

Hickling, A.; Denaro, A.R. *J. Electrochem. Soc.* 1958, 105, 265-270.

Hickling, A.; Davies, R.A. *J. Chem. Soc.* 1952, 3595-3602.

Hickling, A.; Linacre, J.K. *J. Chem. Soc.* 1954, 711-720.

Hickling, A.; Bockris, J.O'M.; Conway, B.E. *Modern Aspects of Electrochemistry*, Plenum Press: New York, 1971, 329-404.

Hittorf, J.W., *Pogg. Ann.*, 1869, 136, 8.

Jandik P.; Bonn, G. *Capillary Electrophoresis of Small Molecules and Ions*; VCH Publishers: New York, 1993.

Jelenkovic, B.M.; Rozsa, K.; Phelps, A.V., *Phys. Rev.*, 1993, 47, 2816.

Klassen, N.V.; Marchington, D.; McGowan, C.E. *Anal. Chem.* 1994, 66, 2921-2925.

Kocketkov, N.K.; Kudrjashov, L.I.; Chlenov, M.A. *Radiation Chemistry of Carbohydrates*, Pergamon Press: New York, 1979.

Kuzuya, M.; Piepmeier, E.H. *Anal. Chem.*, 1991, 63, 1763.

Marcus, R.K., *Glow Discharge Spectroscopies*, Plenum Press: New York, 1993.

Maxfield, F.A.; Benedict, R.R. *The Theory of Gaseous Conduction and Electronics*, McGraw-Hill: New York, 1941.

McLuckey, S.A.; Glish, G.L.; Asano, K.G.; Grant, B.C. *Anal. Chem.*, 1988, 60, 2220.

Miller, J.M. *Chromatography: Concepts and Contrasts*, John Wiley & Sons: New York, 1988.

Nasser, E. *Fundamentals of Gaseous Ionization and Plasma Electronics*; Wiley-Interscience: New York, 1971.

Ohls, K.; Flock, J.; Loepp, H. Fresenius *Z. Anal. Chem.*, 1988, 332, 456.

Parriott, C.; Parriott, D. *A Practical Guide to HPLC Detection*, Academic Press: San Diego, 1993; Chapter 9.

Paulson, J.C. *TIBS*, 1989, 14, 272-276.

Paulus, A.; Klockow, A. *J. Chromatogr.* A 1996, 720, 353-376.

Penning, F.M. *Electrical Discharges In Gases*, Macmillon Co.: New York, 1957.

Petrovic, Z.Lj.; Phelps, A.V. *Amer. Phys. Soc.* 1993, 47, 2806-2822.

Phelps, A.V.; Petrovic. Z.L.; Jelenkovic. B.M., *Phys. Rev.*, 1993, 47, 2825.

Phillips, G.O. *Nature*, 1954, May, 1044-1045.

Phillips, G.O. *Rad. Res.* 1963, 18, 446-460.

Phillips, G.O.; Moody, G.J.; Mattok, G.L. *Rad. Res.* 1958, 3522-3534.

Phillips, G.O.; Griffiths, W.; Davies, J.V. *J. Chem. Soc.* (B), 1966, 194-200.

Piepmeier, E.H.; Cook, B. *Anal. Chem.* 1991, 63, 1763-1766.

Pitkethly, R.C. *Anal. Chem.*, 1958, 30, 1309.

Rassi, Z.E. *Carbohydrate Analysis. High Performance Liquid Chromatography and Capillary Electrophoresis*, Journal of Chromatography Library, Vol. 58, Elsevier: New York, 1995.

Ratliff, P.H.; Harrison, W.W. *Spectrochim. Acta* 1994, 49B, 1747.

Sargent, F.P.; Gardy, E.M. *Canad. J. Chem.* 1976, 54, 275.

Scott, R.P.W., *Liquid Chromatography Detectors*, 2nd ed.; Elsevier: New York, 1986.

Sharon, N.; Lis, H. *Sci. Amer.* 1993, January, 82-89.

Smith D.L.; Piepmeier, E.H. *Anal. Chem.* 1994, 66, 1323-1329.

Smith, B.W.; Womack, J.B.; Omenetto, N.; Winefordner, J.D. *Appl. Spectrosc.*, 1989, 43, 873.

Smith, B.W.; Omenetto, N.; Winefordner, J.D., *Spectrochim. Acta*, 1984, 39B, 1389.

Smith, D.L.; Piepmeier, E.H. *Anal. Chem.*, 1995, 67, 1084.

Spinks, J.W.T.; Woods, R.J. *An Introduction to Radiation Chemistry*, 3rd ed.; John Wiley & Sons: New York, 1990.

Stefansson, M; Westerlund, D. *J. Chromatogr.* A 1996, 720, 127-136.

Stuewer, D. Fres. J. *Anal. Chem.*, 1990, 337, 737.

Wolfrom, M.L.; Binkley, W.W.; McCabe, L.J.; ShenHan, T.M.; Michelakis, A.M. *Rad. Res.* 1959, 10, 37-47.

Zhao, J.; Zhu, J.; Lubman, D.M. *Anal. Chem.*, 1992, 64, 1426.

Zhubiao, Z: Piepmeier, E.H., *Spectrochim. Acta*, 1994, 49B, 1787.